12-29-2021

Assessment of Vertical Accuracy from UAV-LiDAR and Structure from Motion Point Clouds in Floodplain Terrain Mapping

Andrew Muller
Portland State University

Assessment of Vertical Accuracy from UAV-LiDAR and Structure from Motion Point Clouds in Floodplain Terrain Mapping

by

Andrew Muller

A thesis submitted in partial fulfillment of the
requirements for the degree of

Master of Science
In
Geography

Thesis Committee:
Jiunn-Der Duh, Chair
Martin Lafrenz
David Banis

Portland State University
2021

Abstract

Remote sensing technologies are being applied to a variety of uses because of the increase in access to various products (digital sensors, UAVs, software) and its ability to model relatively large areas in a short amount of time. While these new technologies are beginning to be adopted, validation of their merit in floodplain terrain mapping is lacking. The main goal of this study is to evaluate the vertical accuracy of digital elevation models (DEMs) generated with UAV-based LiDAR and Structure from Motion (SfM), also known as photographic LiDAR or PhoDAR. Airborne (manned aircraft) LiDAR has been applied to river research in several applications and is common in many fields such as mining, archeology and surveying. SfM has been used to create digital surface models (DSMs) and DEMs of river systems and their associated riparian areas. Given the foundational difference between LiDAR and SfM technologies, the effects of vegetation on the floodplain landscape required a systematic evaluation to determine which techniques are appropriate for floodplain terrain mapping. We collected remotely sensed data from UAV LiDAR and SfM methods at four field sites located within the interior Columbia Basin and analyzed the resulting point clouds and DEMs to determine their vertical accuracy by comparing their elevations with ground surveyed data (checkpoints) throughout the study areas. Both LiDAR and SfM point clouds were filtered and the remaining ground points were compared to surveyed elevations both in their raw form and interpolated DEMs to assess their vertical accuracy. The results show that in vegetated ground cover, LiDAR point clouds were able to produce higher

accuracy returns and a resulting higher accuracy DEM than SfM results. In non-vegetated areas, the accuracies between SfM and LiDAR returns are closer but still show higher accuracy from LiDAR point clouds. Ground filtering is shown to be a limitation on DEM vertical accuracy because of the inclusion of non-ground points in the filtering process. This limitation impacts the vertical accuracy of both LiDAR and SfM interpolated DEMs in floodplain habitats.

Acknowledgements

I would like to acknowledge and thank the people who helped me complete this project. First, thanks to my advisor, Geoffrey Duh, for his help with planning data collection and analysis. His tireless support and guidance helped me throughout this entire process. Thanks to my committee members, Martin Lafrenz and David Banis, for their feedback and contributions. Thank you to Andrés Holz for his help in planning this project and providing feedback. Thank you to the people who helped with data collection and processing: Derek Arterburn for his help collecting ground data, Kai Ross for his help with processing and R expertise, and Chris Clark for his help and support flying and driving around in the scorching heat as well as getting this project started. Chris, I could not have done this without you. Lastly, thank you to Allyson Will for her help and support throughout this entire process, you have helped me tremendously.

Table of Contents

List of Tables

List of Figures

Chapter 1

Introduction

Remote sensing of river systems and their associated floodplains has been of interest for several years because of the ability to assess relatively large areas with fine-scale detail. Several techniques, both ground-based (total stations, terrestrial laser scanning) and remotely sensed (manned aircraft), have previously been investigated and the potential benefits of each are well documented (Bangen et al. 2014, Fonstad et al. 2013). Recently, the expansion of unmanned aerial vehicles/systems (UAV/UAS) has led to an increase in interest for applying remote sensing to a multitude of fields, with floodplain monitoring among them. The expansion and interest in UAVs has been increasing at an even greater rate since the adoption of commercial flight regulations from the Federal Aviation Administration in 2016 that simplified the process of commerical UAV flight. At the same time these remote sensing systems have been evolving and are now relatively widespread in their adoption. We are currently at the confluence of relative ease to obtain commercial UAV licenses and remote sensing systems that are becoming widely available. While remote sensing is increasing in popularity, validation of its accuracy in a variety of landscapes and ecosystems has not been completed. My research focuses on the vertical accuracy of both UAV- Light detection and ranging (LiDAR) and UAV-Structure from Motion with Multi View Stereo (SfM-MVS) throughout several floodplain restoration projects within the interior Columbia Basin.

Floodplains and their associated river systems are commonly studied for restoration and environmental monitoring in general. River and floodplain restoration projects are completed on a global scale and have become increasingly common in North America. Floodplain restoration is undertaken for the need to store water during periods of high flows to alleviate flooding as well as provide habitat to species such as salmon and steelhead. This project was completed in conjunction with a larger floodplain monitoring protocol implemented throughout the Columbia River Basin by Bonneville Power Administration that has previously relied on ground-based surveys to monitor river and floodplain restoration projects. The Action Effectiveness Monitoring (AEM) Program was developed to address the need for restoration project-level monitoring to quantify its effectiveness (Bonneville Power Administration 2014).

Digital Elevation Models (DEMs) of floodplains are utilized in several manners. Prior to restoration implementation, pre-restoration conditions are mapped to assess baseline conditions. Commonly, after restoration is completed, DEMs are created to compare topographic changes from the restoration efforts. This technique, creating DEMs of Difference (DODs) to assess changes in topography is utilized in restoration monitoring and geosciences in general (Westoby et al. 2012).

Typically, ground based surveys of floodplains are completed using survey equipment such as total stations to collect topographic information and create DEMs of the project areas. In recent years, with the remote sensing technologies becoming more common, there has been an interest in utilizing remote sensing to complete or accompany the traditional ground-based surveys (Bangen et al. 2014). Floodplains are particularly

difficult to survey via ground-based methods because of their size and complex topography. Current floodplain monitoring via ground-based surveys includes topographic point collection within the stream channel. This analysis and recommendations focus on the non-wetted area because of the inability of LiDAR and SfM to accurately capture the submerged bed surface. Previous literature has combined remotely sensed DEMs and in-stream ground-based topographic points with success (Roni et al. 2020). As such, this analysis focuses on remotely sensed DEMs and assumes in-stream points would still be collected and merged with remotely sensed DEMs.

Floodplains provide a unique ecosystem to test the accuracy of derived DEMs. The ground cover is typically vegetated with some areas, mainly exposed gravel bars, being clear from vegetation. Having a variety of ground cover allows for us to analyze the vertical accuracy associated with several ground cover types. The study areas encompass differing floodplain types, from floodplains featuring little tree cover with dense ground vegetation and open, unobstructed stream banks to others featuring mature tree cover, dense ground vegetation and relatively steep banks along some of the study area. The variety of vegetation cover and land characteristics help this study by allowing for accuracy analysis in differing ecosystem types. Similarly, the complexity of the study areas push the boundaries of both collection methods. Dense vegetation and complex topography throughout all the study areas are testing the limits of both methods. By analyzing the vertical accuracy of point clouds and their associated DEMs, we can see where the limitations are for each acquisition type and further the knowledge of when a particular system will likely meet the needs of practitioners.

LiDAR is an active sensor that emits laser pulses and when combined with a global navigation satellite system (GNSS) receiver and Inertial Navigation System (INS) returns a georeferenced point cloud of the earth's surface. LiDAR technology has been well described in existing literature and I will not be including a detailed overview of its description. For further descriptions of the technology readers are referred to the ASPRS Manual of Airborne Topographic Lidar (Renslow 2012). Much of the existing literature on LiDAR has been focused on manned aircraft (Hodgson and Bresnahan 2004). While the technology and processing are the same as UAV-LIDAR, the resulting point clouds slightly differ. Because UAVs are limited in altitude and flying speed, the point clouds are typically much denser than those obtained from manned aircraft (Kucharcyzk 2017). This typically leads to more pulses reaching the ground surface and thus, a more accurate estimation of the earth’s surface. LiDAR has been widely adopted for earth surface modeling because of the ability of its pulses to penetrate through vegetation and collect ground surface returns. The ability to collect multiple returns allows LiDAR data to produce models of digital terrains both above surface features (i.e., digital surface model or DSM) and the bare earth surface (DEM).

Structure from Motion with Multi View Stereo (referred from hereon as SfM) is a form of photogrammetry that reconstructs three dimensional objects from overlapping imagery. Much of the interest in SfM derived DEMs comes from the low-cost of acquisition and ease of processing (Carrivick et al. 2019). SfM was originally designed for 3D reconstruction of objects from random, overlapping photographs. The technology has since been applied to landform reconstructions because of its ability to create 3D

models with nothing more than an off-the-shelf camera. In a broad sense, SfM builds 3D models by looking for matching features in overlapping imagery in a similar process to traditional photogrammetry. For a full review of the technologies and process I refer readers to Snavely et al. (2006). Once processed, SfM returns a point cloud with similar attributes to LiDAR. Given the similarity in the point cloud representation, SfM is also known as photographic LiDAR or PhoDAR. However, since SfM is based on optical images and does not have the "canopy-penetration" capability, its digital terrain model only captures the elevation above surface features (i.e., DSM). Because of the inability of SfM-MVS point clouds to penetrate vegetation, above ground features are included and thus, their representations are a DSM. With the exclusion of above ground features through filtering of the point clouds to approximate the earth's ground surface, the models can be referred to as a DTM or DEM; I will be using the term DEM to refer to the ground representation for both LiDAR and SfM results in this analysis.

Whether to utilize UAV-LiDAR or SfM has been examined in the literature (Simpson 2018, Kucharczyk 2017). The strengths and limitations are well known for both techniques as well. The main benefit of LiDAR is the ability to collect ground returns in vegetated areas. SfM cannot return ground elevations in vegetated areas because the point clouds are built upon the spectral information that is returned in the photos. It is generally accepted that SfM is limited by vegetation and cannot accurately return ground elevations in vegetated areas. Previous studies are conflicted on the accuracy of SfM DEMs in river systems but the accuracy is dependent on the collection methods as well as ground cover (Dietrich 2016, Rusnak et al. 2018). However, it is not known what the limit of

vegetation density and height is and when SfM can be utilized to reasonably model the earth's surface. The unknown limitation is part of the focus of this research, as well as the accuracy of the derived DEMs when compared to LiDAR DEMs of the same study areas.

Prior to the UAV-LiDAR and SfM point clouds being processed into DEMs, ground points must be extracted from the entire cloud. This process has been explored in previous literature and can be completed using several different, although mostly similar, algorithms (Tan et al. 2018, Yilmaz et al. 2021). Some of these algorithms are within closed-source software, such as ArcGIS (ESRI 2020) and ENVI (L3 Harris Geospatial 2021), as well as open-source software packages, such as MCC (Evans and Hudak 2007) and CSF (Zhang et al. 2016). Previous literature has examined the results of various ground filtering (the removal of non-ground points) algorithms on DEM accuracy and found varying results depending on terrain type and collection type (Yilmaz et al. 2018, Zeybek 2019, Klapste et al. 2020). Yilmaz et al. (2018) and Zeybek (2019) found the CSF algorithm to provide the highest accuracy DEMs compared to other commercial and open-source filtering algorithms while Klaptse et al. (2020) found the CSF algorithm provided the lowest accuracy results. Determining the ground points is an important step in the creation of DEMs and DTMs but is somewhat overlooked by common practitioners and is a key step in model accuracy. Some ground-filtering algorithms have little or no room for altering parameters while others, CSF in particular, allow the user to adjust parameters and affect which points are determined to be ground points. This step is subjective in nature and is difficult to perfect, especially in heavily vegetated or sloping terrain. Over a continuous study area, the algorithm is tasked with deciding which point

returns are vegetation and which are ground returns and can be mixed up because steep slopes or banks can mimic the appearance of vegetation and vice-versa, with vegetation appearing to the algorithm as ground features. Ground filtering algorithms were built for classifying LiDAR point clouds, and the differences in characteristics between SfM and LiDAR point clouds can further add to the processing issues inherent within filtering. Recently, Klapste et al. (2020) examined the effects of different filtering algorithms and their parameters on SfM and LiDAR point clouds and found that LiDAR point clouds exhibited more consistent results than SfM. The effects of ground filtering parameters and point cloud densities are examined in our discussion and provide opportunities for future research.

The specific goals of this project are to: 1) assess the vertical accuracy of UAV-LiDAR and SfM point clouds in the context of floodplains 2) assess the vertical accuracy of UAV-LiDAR and SfM derived DEMs and 3) give recommendations to future practitioners about each technique.

Chapter 2

Study Areas

2.1 Site Locations

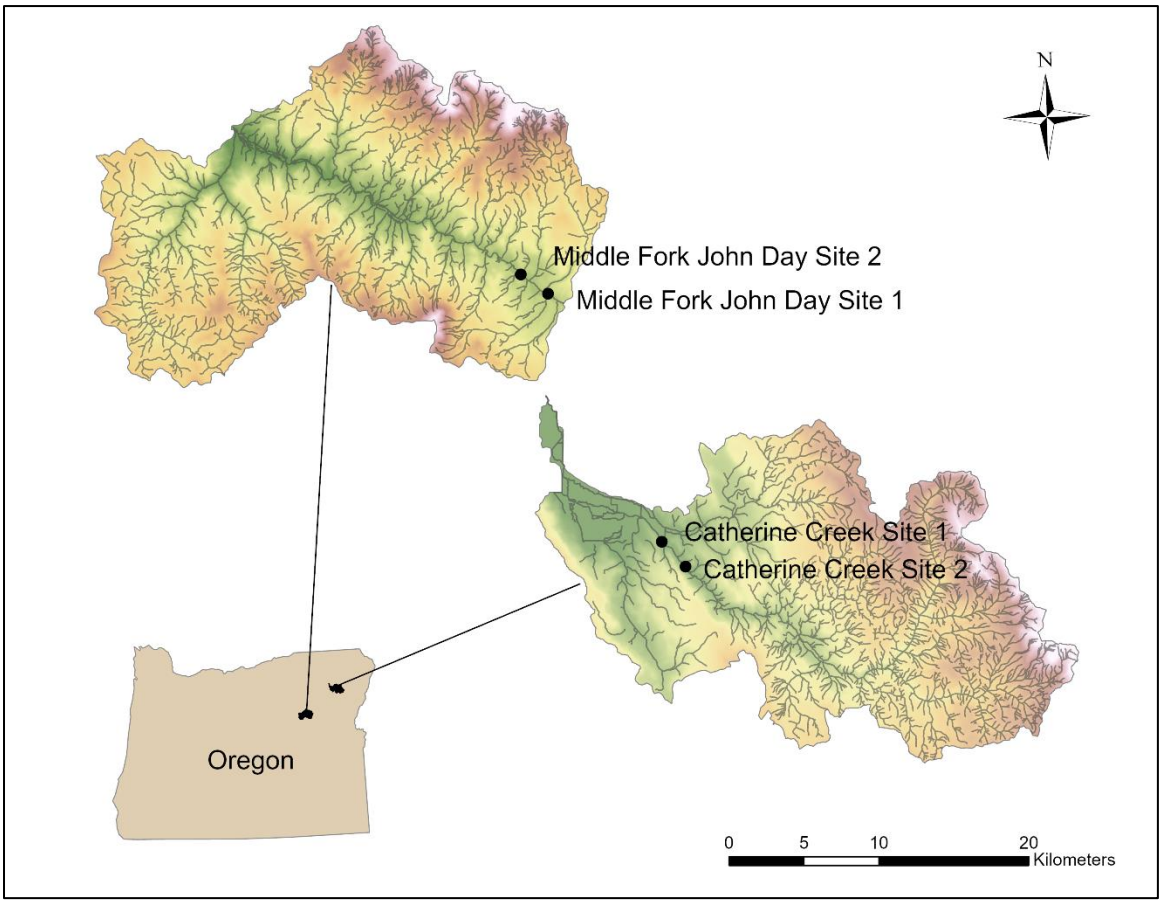

Figure 1. Overall Site Locations.

The selected sites range in characteristics from what can be considered likely to be successful for both techniques to sites that challenge both techniques. In all, four sites were used in this analysis, two sites on the Middle Fork John Day River in Northeast Oregon (MFJD 1 and 2, figures 2 and 3) and two sites on Catherine Creek, a tributary to the Grande Ronde River in Northeast Oregon (CC 1 and 2, figures 4 and 5).The sites were located within the interior Columbia Basin (east of the Cascade crest) with four separate locations on two different rivers with stream length ranging from 360-930 meters (Figure 1). Sites were paired as a treatment and control for the floodplain restoration monitoring project and are therefore meant to be closely matched at each pairing for consistent environments (gradient, vegetation coverage, stream channel width, etc.). The treatment locations featured additional in-stream large wood structures and floodplain reconnection such as newly created side channels.

2.2 Site Characteristics

Figure 2. Middle Fork John Day Site 1.

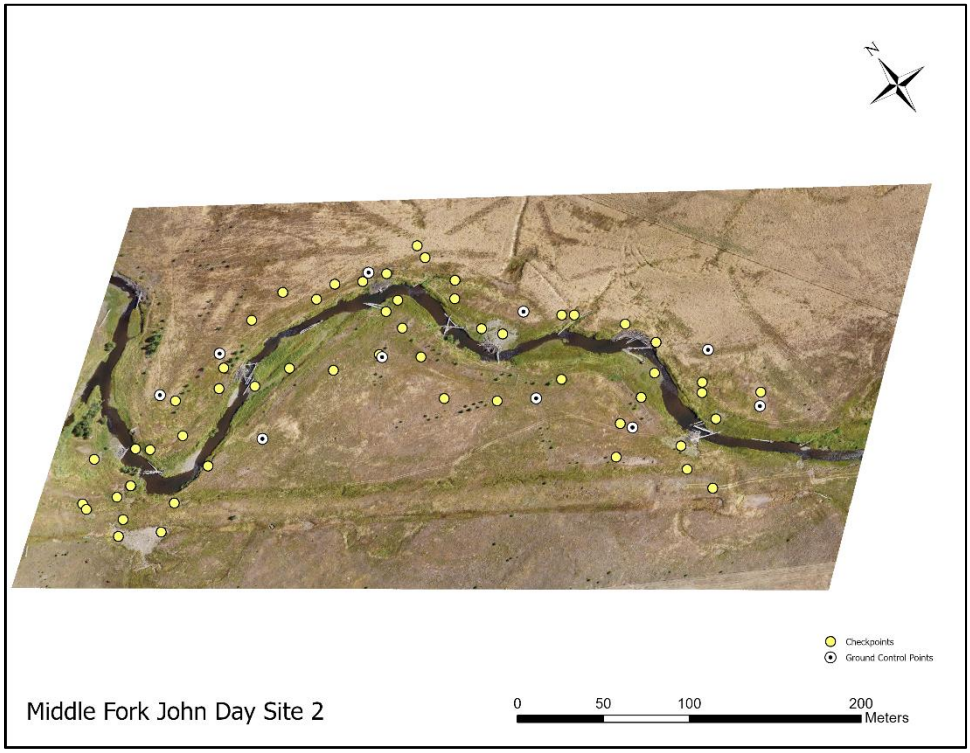

Figure 3. Middle Fork John Day Site 2.

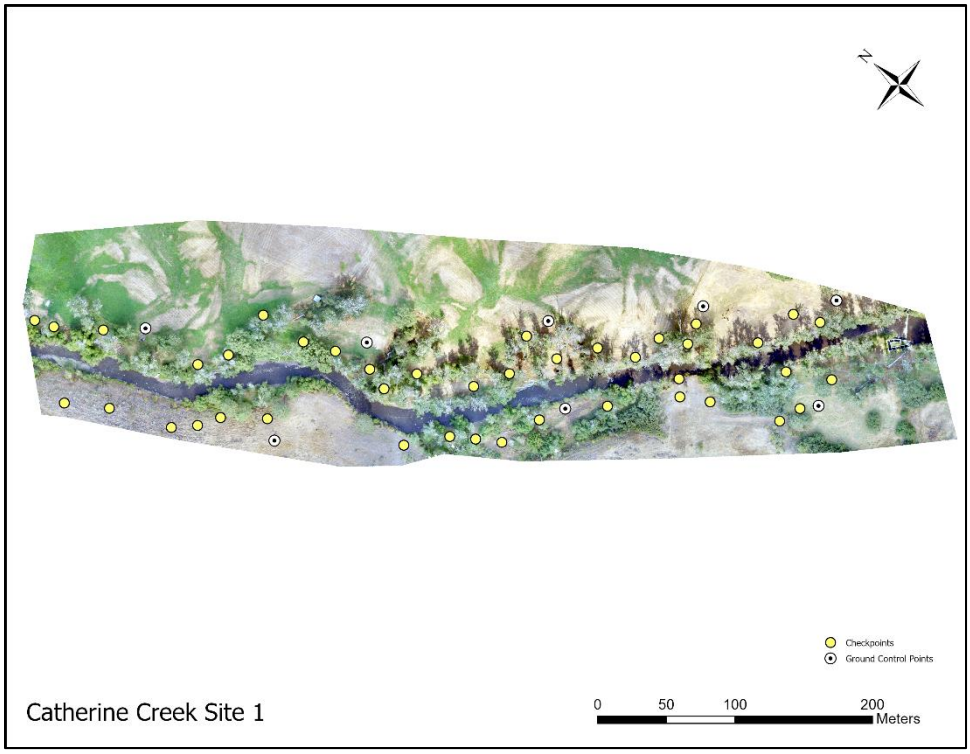

Figure 4. Catherine Creek Site 1.

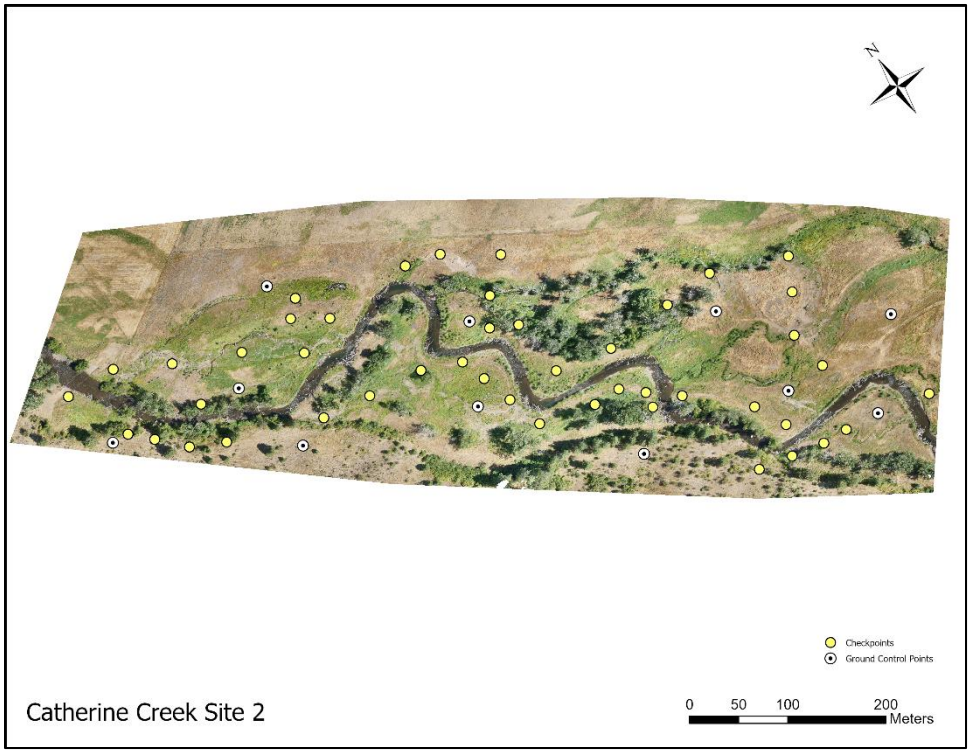

Figure 5. Catherine Creek Site 2.

The four independent sites can be grouped together into two overarching categories because of the similarities between the sites at each grouping. Area 1, the Middle Fork John Day, has minimal conifer (Ponderosa Pine, *Pinus Ponderosa*) tree cover (no trees over 5m in height at both locations) with no deciduous trees present. The sites feature a broad valley with an unconfined channel except for the upstream end of MFJD 1 where the channel is confined against the road prism along the north bank for approximately 40 meters. The ground cover features dense grasses that are grazed by livestock but had minimal livestock grazing signs present at the time of data collection. Exposed gravel bars and dry side channels are also featured at the site as a minimal

percentage of overall ground cover. The overall gradient is very low and the stream channel features a series of pool and non-turbulent habitat types.

Area 2, Catherine Creek, includes a mix of conifer (Ponderosa Pine, *Pinus Ponderosa)* and deciduous (Cottonwood, *Populus Trichocarpa*) trees mainly in the riparian corridor, with Ponderosa also along the upland reaches on the margin of the site extent. The sites feature a broad valley along the north bank with the channel intermittently confined against the hillslope along the south bank at both reaches. The north bank features little slope topography while the south bank has a relatively steep slope. Site 2 features a variety of ground cover types, with grasses dominating the overall ground cover. Exposed gravel bars and dry side channels are also featured at these locations. CC 2 features no known cattle grazing while CC 1, which is on private land, features livestock grazing on both cultivated land and upland dryland habitats. The ground cover at CC 1 features a combination of classes, with recently mowed planted cover crops, upland sage steppe with intermittent shrubs and grasses among exposed earth and livestock fenced areas with livestock present at the time of data collection.

Chapter 3

Data Collection

3.1 Post Processing Kinematic (PPK) Data Collection

The initial data collection began with a post processing kinematic (PPK) global navigation satellite system (GNSS) survey for checkpoint and ground control point (GCP) collection. The data colleced at the check points were for vertical accuracy analysis and the GCPs for geo-referencing the images that were used in SfM. There were several individuals involved in the data collect efforts. They are Derek Arterburn and Christopher Clark. The PPK equipment used were two Trimble R10 GNSS units, one to log as a base station on an autonomous point location (base) and another to collect the checkpoint and GCP locations (rover) (Figures 6 and 7). A minimum of 10 GCP's were placed throughout each study area with relatively large spacing between each and away from the edge of the study area in order to minimize errors. Data was collected and post-processed after sending the base station information to National Geodetic Survey's Online Positioning User Service (OPUS) and correcting the rover point data (National Geodetic Survey 2020). There are several ways to collect and process checkpoint and GCP locations; we relied on the Post-Processed Kinematic (PPK) technique for two main reasons. First, our site locations were out of cell phone service range so we could not rely on the Continually Operating Reference Stations (CORS) network to act as a base station and instantaneously correct our survey points. Second, because of the remote nature of the survey locations, known monuments were not within the signal range from the base to

rover. Because of this, we set up the base station on an autonomous point and post-processed both the base station and rover point locations to increase the accuracy and precision of the survey. The workflow to setup the PPK collection is as follows:

1) set up the PPK base station and log points on the static unit. Standard practice has the base station collecting points for 30 minutes prior to topographic point collection. The base station is set to log at 1Hz and collect a point every 15 seconds.

2) After 30 minutes, the base station has logged enough location information to accurately proceed.

3) Rovers are set to collect point location (UTM NAD83 Zone 11N) as well as attributes about the point (vegetation characteristics), with the following information collected at each checkpoint:

    a) Land Cover (Yes/No)

    b) Vegetation Less Than 1 Meter (Yes/No) – if Yes – Vegetation Type

    c) Vegetation Between 1-5 Meters (Yes/No) – if Yes – Vegetation Type

    d) Vegetation Greater Than 5 Meters (Yes/No) – if Yes – Vegetation Type

Figure 6. PPK Data collection - Rover and Base Station.

Figure 7. GCP marker. The diameter of the marker is 30 cm.

3.2 SfM and LiDAR Collection

SfM and LiDAR data were collected simultaneously on the same UAV flight and processed separately in two distinct pipelines. The camera was mounted to the rear of the LiDAR unit with a fixed mounting bracket that forced the camera to strictly record imagery at a nadir angle (Figure 8). Flights were conducted immediately following the collection of PPK topopgraphic points in late August and early September of 2019. To begin each survey, the INS must start alignment in a steady state on the ground with no movement for a minimum of five minutes. After the initial alignment, the flights began with an out and back straight-line flight away from the operator for approximately 50 meters then a series of figure eight turns were completed to further align the INS. The INS alignment data was sent to the laptop via the LAN network so the survey technician can assess the quality of INS alignment prior to data collection. Once the INS was aligned and uncertainties in the location data were minimal the operator is ready to fly to the first survey waypoint. The survey technician then triggered the camera via the LAN connection to begin collecting data. Once the flight was completed the survey technician then triggered the camera and LiDAR sensor to stop recording and the final INS alignment procedures were completed. After a five-minute wait time to finalize the INS alignment, imagery and initial LiDAR data were then taken off the camera's SD card and stored on an external hard drive.

Figure 8. UAV Mounted with LiDAR and SfM Camera sensors. The camera and LiDAR sensor are both mounted to a fixed bracket.

3.3 LiDAR Sensor Specifications

A Velodyne VLP-16 LiDAR sensor (a dual return, 16 laser sensors with a maximum range of 150 m) customized by Phoenix LiDAR was affixed to the DJI m600 for LiDAR flights. When maintaining a flight altitude of 50 m and a speed of 8 m/s, this sensor is reported to return a point density of approximately 225 points per square meter.

3.4 SfM Camera Specifications

Photos were captured with a Sony A6000 digital camera in RAW 14-bit format. This camera has a full frame sensor (CMPS APS-C [23.5 x 15.6 mm]) and a 16mm Prime f/2.8 lens. Settings were placed on auto for shutter speed and ISO. The camera was

mounted to the LiDAR unit with a fixed bracket that forced the camera to strictly record imagery at a nadir angle.

3.5 Flight Planning

I used Phoenix LiDAR's flight planner software to create and download flight plans (Phoenix LiDAR 2020). The flight plan kml files were then uploaded into Litchi, a flight application that is used for DJI aircraft (Litchi 2020). Flight speed was set at 8 m/s and overlap was set at 80% side and front to prevent any gaps in imagery or point clouds. Figure 9 shows the flight lines at MFJD Site 2.

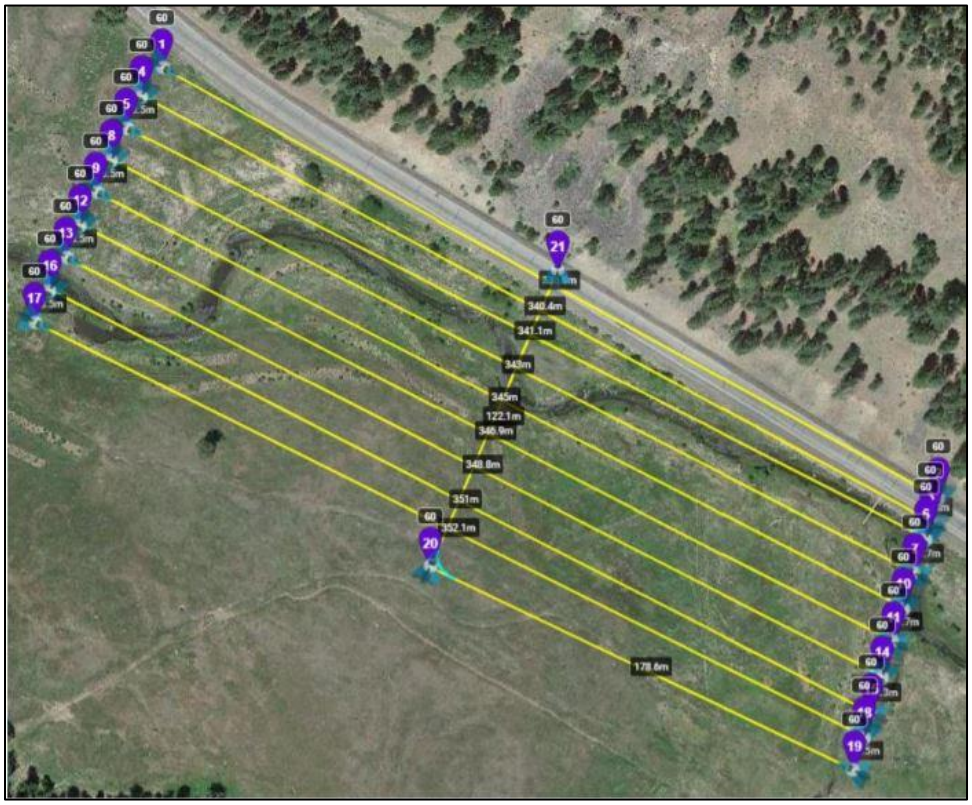

Figure 9. Flight Plan for Middle Fork John Day Site 2.

Chapter 4

Processing

4.1 GNSS Point Processing

GNSS points were collected at GCP and checkpoint locations throughout each site. After collection the point files were processed in Trimble Business Center (TBC) using the base station .to2 file to correct the rover point locations (Trimble 2020). As discussed previously, the point locations were processed as PPK because of limitations at our site locations. Base files were corrected using OPUS then imported into TBC to apply corrections to the collected points. The coordinate system is set as NAD83(2011) UTM Zone 11N and the vertical datum is NAVD88 (Geoid 12B). Computed vertical precision from TBC is reported at the 95% confidence level with the average precision of .025 m and a standard deviation of .012 m.

4.2 SfM Processing

I performed SfM processing using Agisoft Metashape Version 1.5.5 (2020). Photos were collected in ARW format, Sony's RAW image format. Metashape does not support uploading images in RAW format, and only accepts JPEG or TIFF formatted pictures. The Sony a6000 captures raw images in 14 bit, meaning there are 2 to the 14th power tone combinations (16384). RAW images were converted to JPEG using Sony's

imaging edge software with the highest quality (lowest compression) setting before processing in Metashape.

Once images were converted to JPEG, they were imported into Metashape to begin processing. After importing, I followed the recommendations from Agisoft to produce the highest quality point clouds and orthomosaics. The following is a step-by-step process to produce georeferenced point clouds and orthomosaics:

1) Remove photos that will not be included in the model. These are photos that are collected before and after we reached our survey flight lines and typically included several photos at each site.

2) Estimate image quality for each individual image. The image quality is calculated based on the sharpness of the image at its most focused location. Images with a quality below .5 are recommended to be disabled if the remaining images still cover the entire site.

3) Generate masks. These are only required for objects that I would not want to be included in our model and they can include livestock grazing in the site or vehicles that drove through the site while collecting data. Masks were generated manually and few were required throughout the study areas.

4) Align photos. Settings vary based on processing time, the highest setting uses the original photo size, medium setting downscales the image by a factor of 4 and low downscales by a factor of 16. The following settings were used: High, key point limit of 40,000, tie point limit of 4,000, adaptive camera model fitting: Yes.

5) Import ground control points (GCP's). GCP locations are imported into Metashape in .csv format with the same coordinate system as the project settings (NAD83, UTM). The .csv contains columns for the GCP ID number, easting, northing and elevation.

6) Locate GCP targets in images. Images that contain the GCP targets (Figure 7) are selected and the correct GCP number is selected from the list of imported coordinates. Once a GCP has been selected in two images, they are then added to all the images that contain that location. The GCP location is then verified for all photos and adjusted if necessary.

7) Optimize camera alignment. During georeferencing the model is linearly transformed and possible non-linear deformations can be removed by optimizing the point cloud and camera parameters from the known GCP locations.

8) Build a dense point cloud. Similar to step 4, settings vary based on processing time. The difference is that the Ultra High setting uses the original photos and High downscales by a factor of 4. Agisoft does not recommend using Ultra High for larger projects such as ours because of the demand on the computer's RAM. Depth filtering is adjustable, with mild depth filtering leaving the most detail and moderate leaving some but aggressive removing much of the model's detail. The following settings were used: Quality: Medium, depth filtering: mild.

9) Build orthomosaic and generate point cloud DSM. Resolutions of the orthomosaic were approximately 2.5 cm.

4.3 Generating The LiDAR Point Cloud

Corrected base station files, trajectory files and associated raw lidar files were uploaded to Phoenix LiDARMill software to process the raw LiDAR data (Phoenix LiDAR 2020). The exact details of processing within LiDARMill are proprietary, the basic formula takes the raw files, adjusts locations based on boresighting between the sensor and INS then interpolates a 3D position based on the coordinate system being used. After processing, a georeferenced point cloud is exported.

4.4 Point Cloud Filtering

After the point clouds are processed, filtering the point clouds to include only ground points is required. Several variations of this processing technique exist in both open and closed source forms. In order to produce an elevation model that ignores above ground vegetation and objects, the points that encompass the above ground features need to be removed and the ground-surface below the objects interpolated. Studies have shown that filtering algorithms differ in their selection of ground points, with some producing higher accuracy results in flat vs. sloped terrain or vegetated vs. non-vegetated (Yilmaz et al. 2018, Klapste et al. 2020). I tested the Boise State Lab (BCAL) filtering plugin for ENVI LiDAR (L3 Harris Geospatial 2021) and the RCSF filter within the lidR R package (Roussel et al. 2020). After testing multiple filtering techniques, I selected the lidR CSF filter because of its speed in processing, adjustable parameters and open-source format. The cloth simulation filter is an implementation of the CSF algorithm developed by Zhang et al. (2016) and uses the author's original source code. I direct the reader to

Zhang et al. (2016) for a full review of the CSF filtering algorithm. This step is subjective in nature because of the parameter selection that is inherent in the processing workflow; it is likely that individual study areas would require different parameter settings for ideal classification. The parameters that can be adjusted to manipulate the ground points are: Slope (true or false, if true and steep slopes exist in the data, post processing is needed), rigidness (rigidness of the cloth, default is 1), class threshold (the distance of the cloth to classify a point into ground and non-ground, default is .5m), cloth resolution (distance between particles in the cloth, usually set to the average distance of the points in the point cloud, default is .5m), iterations (maximum iterations for simulating cloth, default is 500), time step (time step when simulating the cloth under gravity, default is .65).

Testing the parameters available in the CSF filter is an important step in processing and a sensitivity analysis was performed to determine the ideal settings for our study areas. For this, I adjusted the class threshold and cloth resolution setting in increments of .1, as well as adjusting the slope and rigidness parameters. After the sensitivity analysis was performed, I chose the parameters that are listed in table 1. Klapste et al. (2020) performed a similar analysis on SfM point clouds using a variety of ground filtering algorithms, including CSF, and found that the cloth resolution parameter adjustments had the greatest impact on classification. This is similar to our findings, with cloth resolution deviations from our chosen setting (.2) negatively impacting DEM vertical accuracy to a greater degree than other setting adjustments.

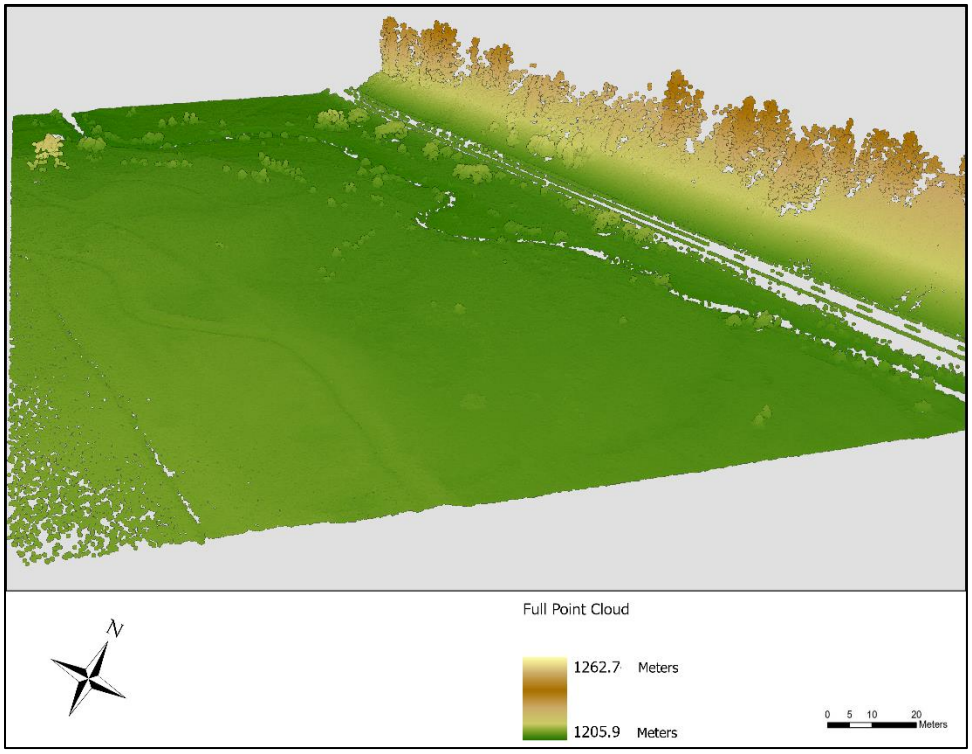

Figure 10. Full Point Cloud for MFJD Site 2.

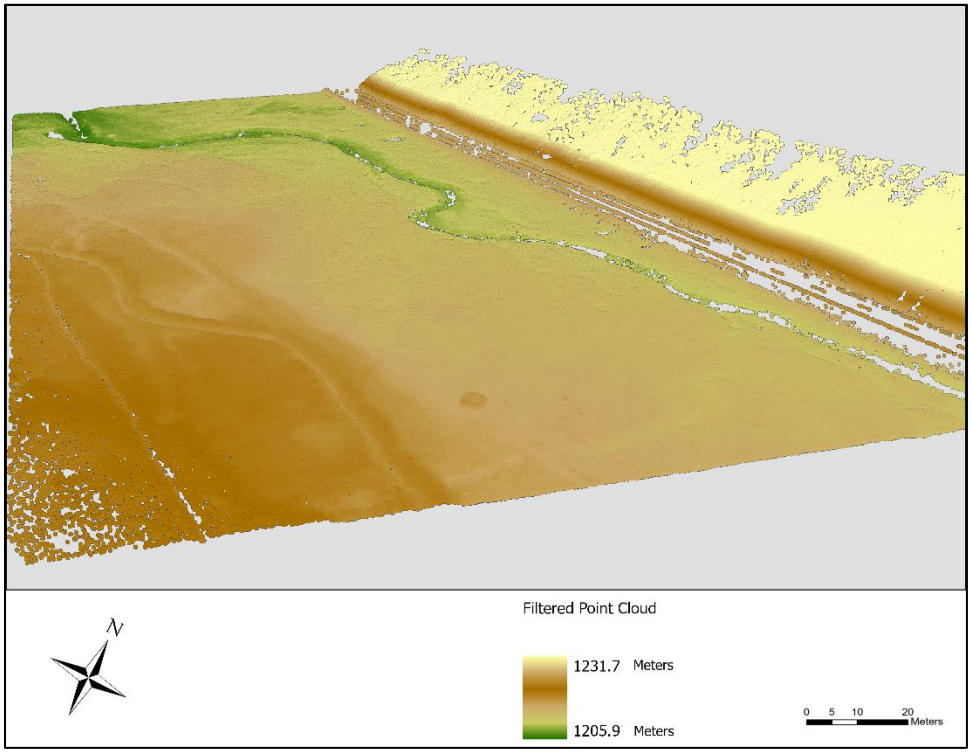

Figure 11. Filtered Point Cloud for MFJD Site 2.

Table 1. Parameter settings chosen for CSF ground filtering algorithm.

Parameter	**Setting**
Slope	False
Rigidness	1
Class Threshold	.5
Cloth Resolution	.2
Iterations	500
Time Step	.65

I decided on mainly default parameters except for the cloth resolution because of the high density of the point clouds being processed. The parameters were unchanged between sites to minimize processing bias. The elevations of the points clouds would not change with parameter adjustments because the filtering does not change the returned value of the point clouds, it only removes points that are deemed as non-ground returns. Figures 10 and 11 illustrate the effect of point cloud filtering. Figure 10 is the original unfiltered LiDAR point cloud from MFJD Site 2. Figure 11 is the filtered LiDAR point cloud using CSF with the tested parameters.

4.5 DEM Processing

DEM processing was performed using the LiDR R package. I chose the k-nearest neighbor with inverse distance weighting (KNNIDW) interpolation method to generate a DEM surface from the filtered point cloud. KNNIDW interpolation is faster than other more complex interpolation methods such as kriging. The settings chosen were default

settings, with the number of nearest k-neighbors equal to 10 and the power for inverse distance weighting equal to 2. The resulting DEMs have a 0.25 meter resolution.

4.6 Reference Data

At each checkpoint collected throughout the study areas land cover attributes within the immediate vicinity (1 meter horizontally or vertically above the ground surface) of the checkpoint were recorded. The land cover and vegetation categories were divided into four discrete groups: Bare earth, vegetation less than 1 meter, vegetation between 1-5 meters and vegetation greater than 5 meters. The analysis was broken into the four land cover categories to test the differences in vertical accuracy between bare earth locations and the vegetated categories. I chose the three vegetation height categories to test whether vertical accuracy is being impacted depending on the characteristics of the vegetation itself. First, to see the influence of grasses on vertical accuracy, I chose the vegetation category of less than 1 meter. Next, to see the influence of shrubs and shorter trees, both deciduous and coniferous, I chose the category of vegetation between 1-5 meters. Lastly, to see the influence of mature tree cover on vertical accuracy, I chose the category of vegetation greater than 5 meters. These categories are not site-specific and could apply to most vegetated sites where remotely sensed UAV data is collected.

The vertical accuracy of the processed datasets were compared to our reference data, checkpoints, taken throughout each study area. ASPRS has published guidelines for vertical accuracy assessment such as number of checkpoints, distribution, and locations (ASPRS 2015). I followed these guidelines wherever possible but were somewhat limited by the existing ground conditions. Bare earth points, with no vegetation present within 1-

meter surrounding the checkpoint, were difficult to find at most sites and were not present at all at one site (MFJD 1). Their distribution was limited to areas immediately adjacent to the stream channel and mostly consisting of gravel bars. Therefore, the spatial distribution and total number of bare earth points was limited but still allowed for analysis. Similarly, two of the four study areas contained no vegetation greater than 5 meters in height so the number of associated checkpoints is lower than other vegetation categories. Table 2 shows the breakdown of points for each category of data collected.

Table 2. Checkpoint Totals by Category

Point Type	**MFJD Site 1**	**MFJD Site 2**	**CC Site 1**	**CC Site 2**	**Total**
Bare Earth	0	26	3	7	36
Vegetation Less Than 1 Meter	21	13	16	23	73
Vegetation 1-5 Meters	4	15	3	7	29
Vegetation Greater Than 5 Meters	0	0	20	9	29

4.7 Vertical Accuracy Assessment

I chose to solely analyze the vertical accuracy of the point clouds and DEMs and not horizontal accuracy for two reasons. First, because of the data collection methods utilizing PPK GNSS survey equipment, the horizontal accuracy of point clouds and resulting DEMs is already known and shown in Appendices A and B. Likewise, the vertical accuracy of the point clouds after ground filtering is unknown and directly impacts the DEM vertical elevations.

The vertical accuracy assessment was performed in two categories: point cloud vertically closest point assessment and DEM assessment. Point cloud terrain data captures the native resolution of the data collection methods, whereas DEM, which contains modified elevation data due to the spatial interpolation process, is a more commonly used terrain model in spatial analysis. To account for the possible misalignment of the geo-referenced data and the inclusion of unfiltered surface features (i.e., above ground vegetation and objects), the vertically closest point assessment used a 5 meter buffer around each checkpoint where the closest 30 points from the respective filtered point clouds were extracted into a shapefile and used for analysis. The closest 30 points elevations were then compared to the checkpoint elevation and the point with the smallest absolute value elevation difference, that is, the vertically closest point, provides the observed elevation value. The horizontal distance from the checkpoint to the said point was calculated for each checkpoint. I expected that the distance varied depending on the site and method, because of the ability of LiDAR to penetrate vegetation more

easily than SfM, the distances for the LiDAR results were smaller than the SfM distances. The checkpoints with denser and taller vegetation have larger distance values than points associated with less dense and shorter vegetation. This is apparent when looking at the vertically closest point for checkpoints associated with vegetation greater than 5 meters, with the average distance being 14.2 centimeters vs. 26.8 centimeters for LiDAR and SfM, respectively. The increased distance associated with SfM is a shortcoming of the approach because of the inability to penetrate vegetation and is pronounced when large, dense tree cover is present.

The reason to perform the vertical accuracy assessment on both the point cloud data and interpolated DEM is to look at the ground-filtered point cloud prior to DEM creation, even though DEMs are the more commonly used terrain representation than point clouds. DEM processing relies on several adjustable parameters that can alter the elevations that are within the model and therefore impact the elevation. The ground-filtered point clouds are not altered in elevation from the original returns, they have only filtered out the points deemed as vegetation or non-ground points. By analyzing the point cloud return elevations prior to DEM creation, I can assess their accuracy without the influence of DEM parameters on elevations. Likewise, I chose to analyze the vertically closest point return instead of the absolute closest point return from the respective clouds because of the known inclusion of erroneous above-ground points in the filtered points clouds.

For initial analysis, I examined the 30 closest point returns to get a sense of the overall differences between each collection method. I looked at the average elevation of

the 30 closest points compared to the checkpoint elevations. Also, I examined the standard deviation of the elevations for the 30 closest points and the range of those elevation values.

To analyze the vertical accuracy of the point cloud returns and the resulting DEMs I first took the extracted vertically closest point return shapefiles at each checkpoint location and calculated summary statistics such as mean, median, standard deviation, range and root mean square error (RMSE) for the vertical differences between the observed (checkpoint) and predicted (point cloud) elevations. I chose to analyze the results using RMSE because it is a common approach suggested for analysis by ASPRS as well as being utilized in exising literature. RMSE is commonly used to analyze remotely sensed data that is interpolated or compared to existing known values. After creating DEMs from the filtered point clouds, the DEM elevations were then compared to the checkpoint elevations with the same summary statistics.

Chapter 5

Results

5.1 Data Summary

Table 3 summarizes the data file sizes and number of photos taken at each respective site. CC 2, by far our largest site, featured more than twice as many photos as the other site locations. Table 4 shows the point densities both before and after filtering at each site location. After filtering, the point densities are very high, with the lowest density at 149 points per m^2 and the highest at 279 points per m^2.

Table 3. Summary of file sizes and number of photos taken at each site.

Site	LiDAR File Size (GB)	SfM File Size (GB)	# of photos
MFJD1	1.1	.84	291
MFJD2	1.2	.78	327
CC1	1.7	1.8	494
CC2	3.8	2.8	1092

Table 4. Point Cloud densities (points per square meter).

Site	LiDAR Full	LiDAR Ground	SfM Full	SfM Ground
MFJD1	186	181	282	269
MFJD2	150	149	210	208
CC1	205	152	395	236
CC2	261	221	357	279

5.2 General Geometric Characteristics of Neighboring Point Returns Compared to Checkpoints

Table 5 is a summary of the 30 closest points from each checkpoint for each method. As shown, the average distance to both the closest point and the vertically closest point are lower for LiDAR when compared to SfM. The standard deviation and range are lower for SfM when compared to LiDAR. These results are as expected because of the nature of both collection methods. Because of the ability of LiDAR to penetrate vegetation, it is expected that the distance to checkpoints would be less than SfM. With SfM point clouds being interpolated from imagery and their points not penetrating vegetation, the surfaces are smoother than LiDAR and therefore, their range and standard deviation are lower.

Table 5. Summary of the closest 30 points to each checkpoint in centimeters.

Method	**Average Distance to Closest Point**	**Average Distance to Vertically Closest Point**	**Average Vertical Standard Deviation**	**Average Vertical Range**
LiDAR	3.8	14.0	7.0	11.5
SfM	5.6	15.2	2.6	8.8

5.3 Nearest Points and Vertically Closest Neighboring Point

The average distance from the checkpoint to the vertically closest point for the LiDAR point cloud is 14.0 cm and the distance from the checkpoint to the minimum absolute difference SfM point cloud is 15.2 cm. The maximum distance from the checkpoint to the minimum absolute difference is 66.14 cm for the LiDAR and 2.28 meters for the SfM. That SfM distance is from a heavily vegetated area with deciduous

vegetation overhead that created a large gap between the checkpoint location and the ground filtered point. This same point for the LiDAR point cloud had a distance of 50.9 cm from the checkpoint, which is an outlier for the LiDAR point distances (Figure 12).

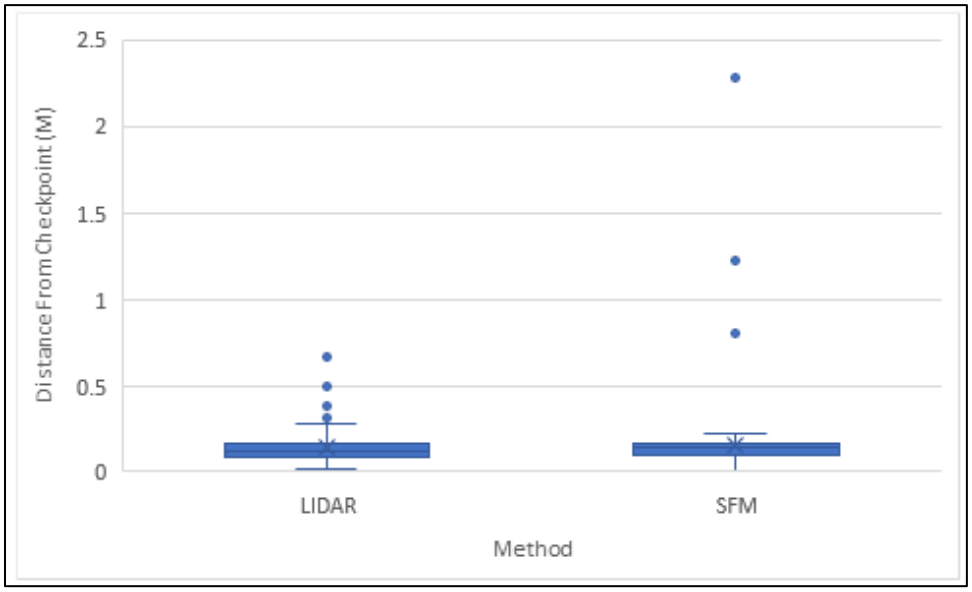

Figure 12. Distance from the checkpoint to the closest point used. SfM average distance is heavily impacted by gaps in the point clouds caused by the presence of vegetation.

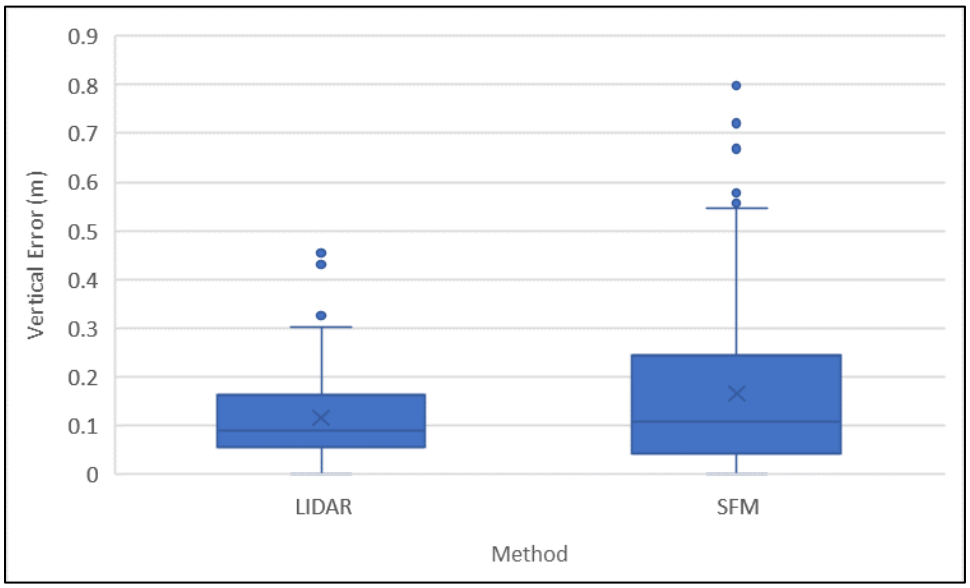

Figure 13. Average of the 30 closest points absolute vertical error compared to the reference data. As shown, outliers in the SfM are negatively impacting the average vertical accuracy. Average vertical errors for LiDAR and SfM are .123 and .163 meters, respectively.

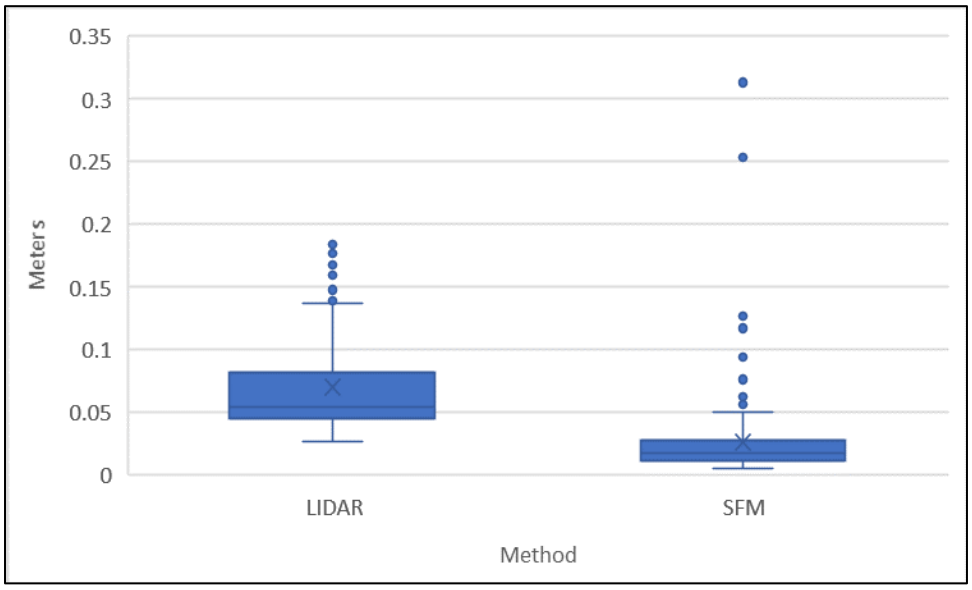

Figure 14. Standard deviation of 30 closest points.

Similar to the distance to checkpoint, the standard deviation for SfM is impacted by outliers from gaps in the point clouds caused by the presence of vegetation (Figure 14). Overall, the SfM standard deviation is lower because of the inherent nature of SfM point clouds being modeled from imagery. In comparison, LiDAR point returns exhibit a much larger range because of their discrete returns and a larger standard deviation is expected. The ranges of the 30 closest point for each method by category are highlighted below (Figure 15). As discussed previously, the ranges for LiDAR are expected to be greater because of the ability to penetrate vegetation. However, despite the ranges for LiDAR being greater their averages are closer to the observed checkpoint elevations.

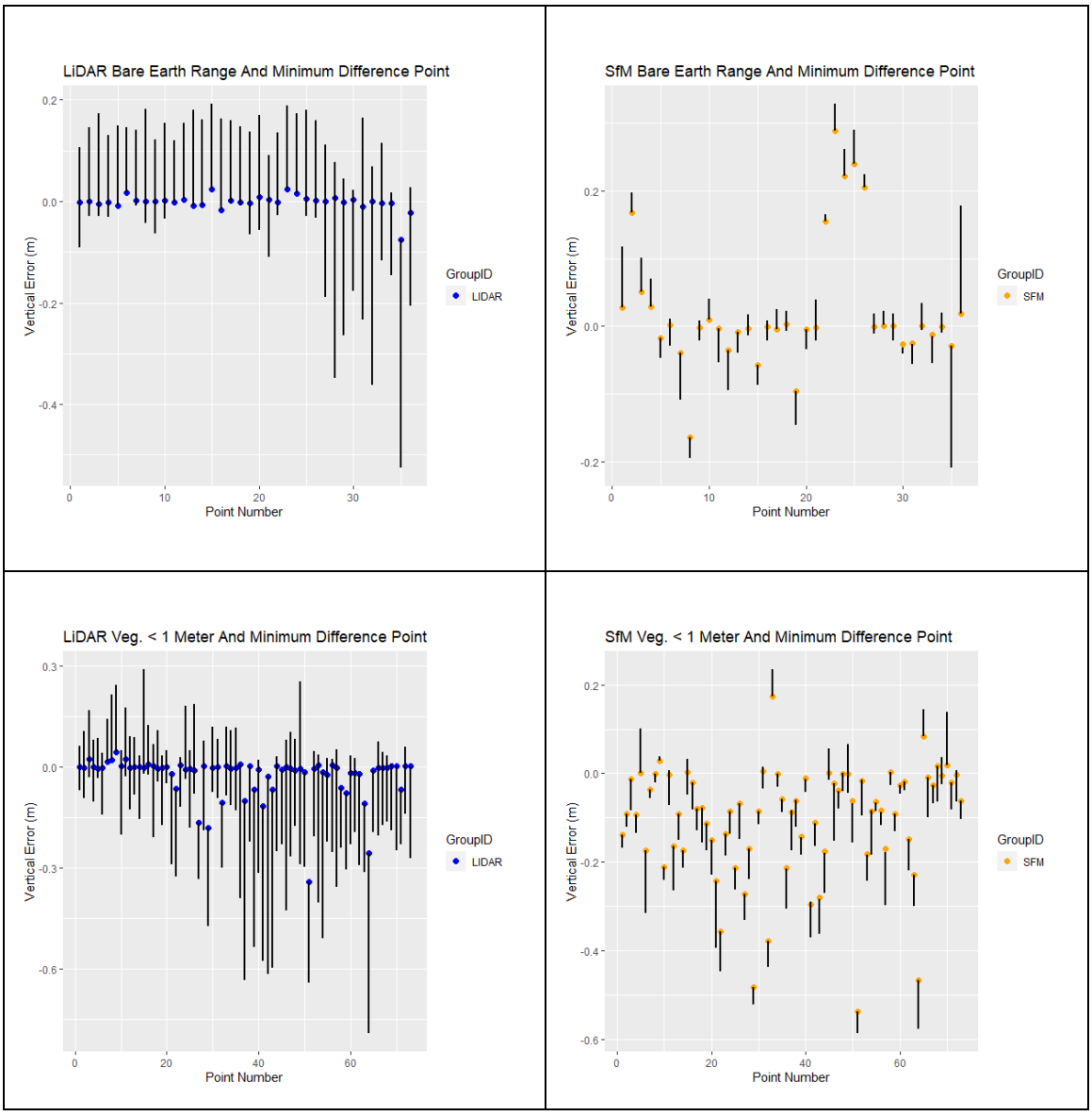

Figure 15. Range of 30 closest point and the vertically closest point for each vegetation class used in analysis. LiDAR has a greater range because of its ability to penetrate vegetation. The SfM range is lower overall but has less accuracy. Figure 15 Continues on the next page.

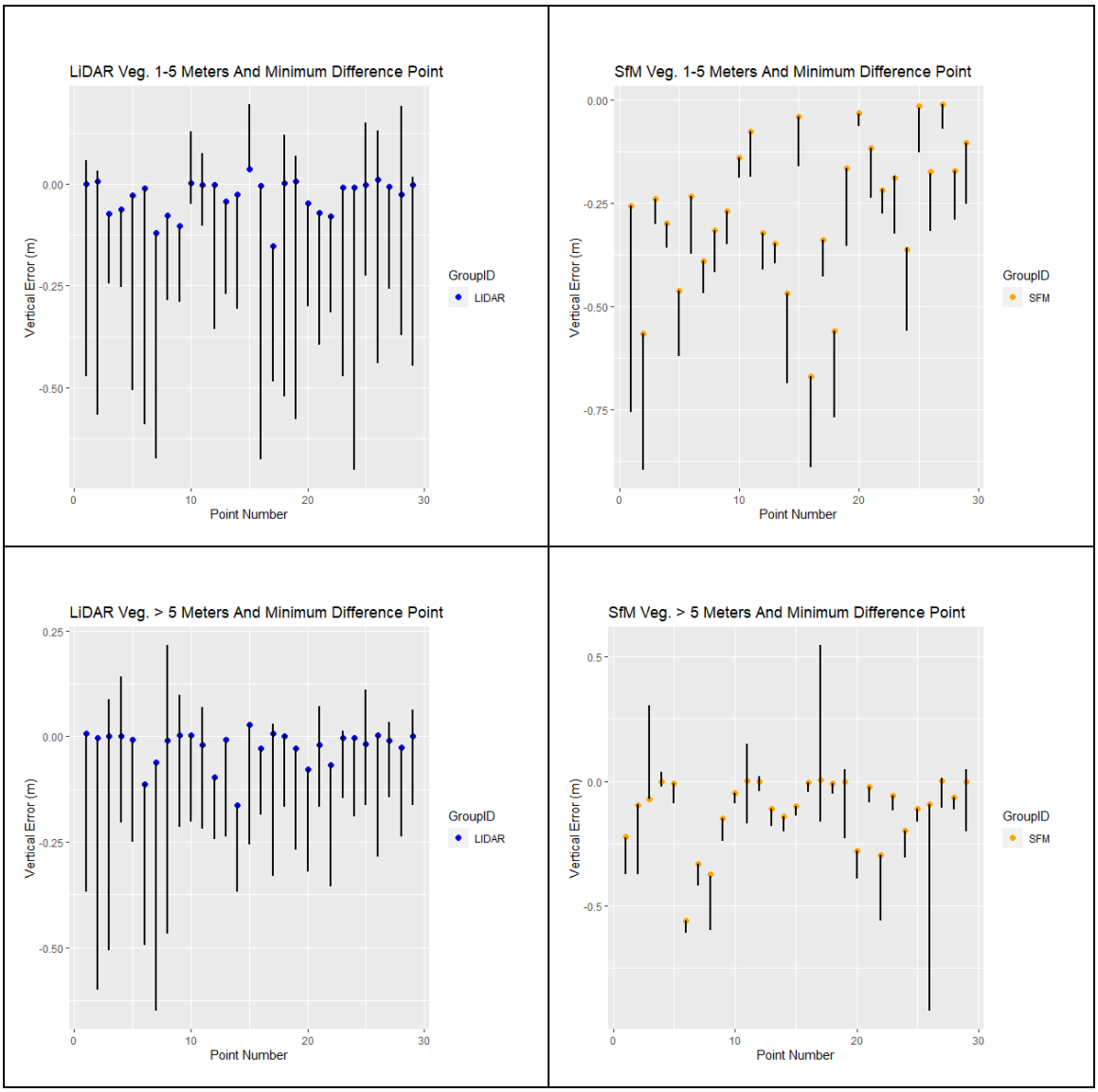

Figure 15 (continued). Range of 30 closest point and the vertically closest point for each vegetation class used in analysis. LiDAR has a greater range because of its ability to penetrate vegetation. The SfM range is lower overall but has less accuracy.

5.4 Vertically Closest Point Results

First, I examined the overall absolute vertical error, that is the observed (checkpoint elevation) minus the predicted (point return elevation) and the results show that the average is much lower for LiDAR compared to SfM (.026 meters vs .126 meters, respectively). Next, I looked at the overall bias of each method. The values represent the overall trend, either underestimating or overestimating the observed elevations, based on method. LiDAR is overall underestimating elevations at the checkpoints to a much less degree than SfM (-.021 meters vs -.105 meters, respectively). Table 6 breaks down the bias by category and shows the differences in bias based on the land cover category. For all categories except SfM bare earth, the point returns are underestimating the checkpoint elevations. Lastly, I analyzed the standard deviation of the vertically closest points when compared to the checkpoint elevations. The deviation is larger with SfM (.16m) compared to LiDAR (.05m) and is mostly caused by outliers impacting the SfM results.

Table 6. Point Cloud Bias by Category (meters).

Method	**Bare Earth**	**Veg <1m**	**Veg 1-5m**	**Veg >5m**
LiDAR	-0.0017	-0.0249	-0.0309	-0.0244
SfM	0.0245	-0.104	-0.2593	-0.1155

5.4.1 Vertically Closest Point Accuracy by Vegetation Category

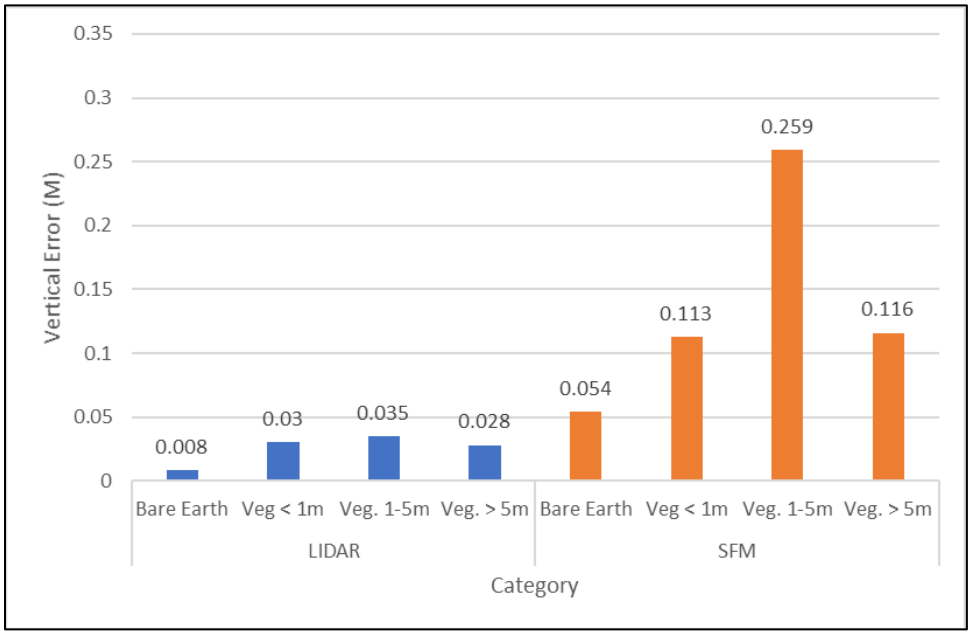

Figure 16. Absolute Vertical Error for all Categories.

As shown in Figure 16, vegetation has a large impact on the vertical accuracy of both SfM and LiDAR point clouds. The highest error is associated with the category of vegetation between 1-5 meters. Both SfM and LiDAR follow similar patterns, with vegetation greater than 5 meters having a similar impact on vertical accuracy as vegetation less than 1 meter. These results are expected because of the known influence of vegetation on vertical accuracy. However, the increased error associated with vegetation between 1-5 meters for SfM was not expected compared to the other vegetated categories. This effect is examined further in section 6 and is likely associated with the ground filtering algorithm.

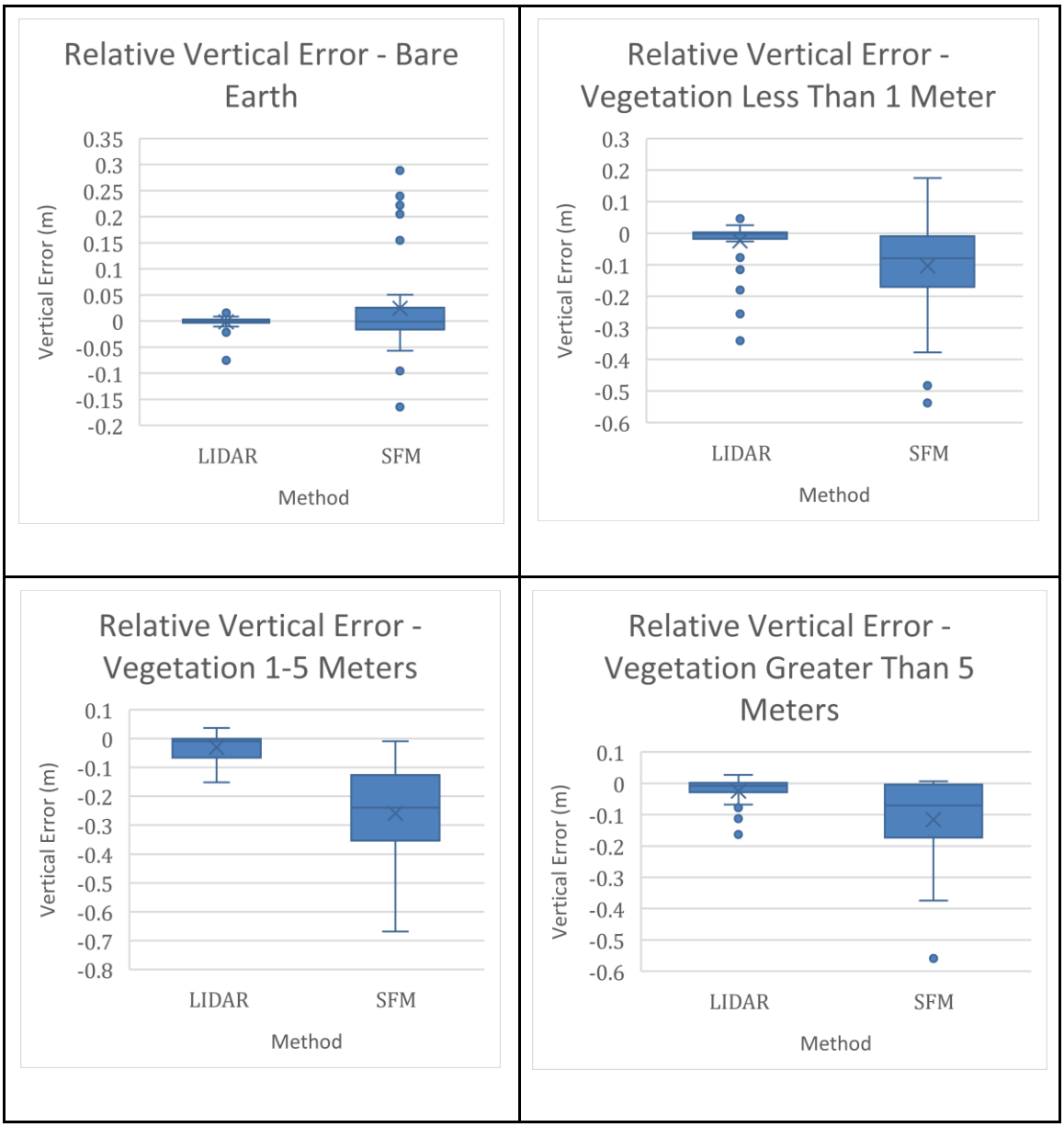

Figure 17. Relative vertical error by category (meters).

As shown in Figure 17, relative error varies by vegetation category but overall, the point clouds are underestimating the elevation (observed - predicted). Bare earth points are the exception, with SfM overestimating the elevation. This is potentially due to the variable terrain conditions at the site locations where a checkpoint elevation could be slightly higher than the surrounding ground elevations.

Tables 7 and 8 show the root mean square error (RMSE) for each category. The RMSE computed at the 95% confidence interval is recommended for analysis by ASPRS (ASPRS 2015) and RMSE results again highlight the influence of vegetation between 1-5 meters on SfM, while not showing the same influence on LiDAR.

Table 7. Point Cloud RMSE by Category (Meters).

	Bare Earth	**Veg <1**	**Veg 1-5**	**Veg >5**
LiDAR	.0155	.0664	.0534	.0483
SfM	.0962	.1651	.3098	.1789

Table 8. Point Cloud RMSE at 95% Confidence Interval (Meters).

	Bare Earth	**Veg <1**	**Veg 1-5**	**Veg >5**
LiDAR	.0304	.1302	.1046	.0947
SfM	.1885	.3236	.6072	.3507

5.5 DEM Vertical Accuracy

The DEM analysis follows the same methods as the vertically closest points analysis and highlights the impact of ground filtering on DEM vertical accuracy. Overall errors are higher than the vertically closest points, which is expected, but are somewhat higher than expected. This increased error is likely influenced by the inclusion of non-ground points in the filtering and is further examined in section 6. The overall vertical error for LiDAR is lower than SfM, as expected, however the error difference is smaller than the vertically closest point results. This is likely explained by the greater range in elevation values from filtered LiDAR returns when compared to SfM. Because the ground filtering algorithm is having difficulty in classifying ground points, and is including some vegetation returns in the results, the larger range in elevation values for LiDAR points are impacting the DEM vertical accuracy to a larger degree than the SfM DEMs. The overall average vertical error is still lower for LiDAR compared to SfM, with the average being .12 meters vs .163 meters respectively. Looking at overall mean bias, LiDAR is closer to the observed elevations (-.08m) compared to SfM (-.13m). Table 10 breaks down the mean bias by land cover category. Overall, SfM is underestimating elevation values to a greater degree than LiDAR. However, as table 9 shows, LiDAR and SfM are both overestimating elevation values for bare earth points. Overall standard deviation of DEM vertical error associated with each method shows results that are similar to the vertically closest point analysis. LiDAR DEM standard deviation is .13m and SfM DEM standard deviation is .19m. These results highlight the impact of outliers on SfM that are caused by vegetation limiting its ability to accurately capture the ground elevation.

Table 9. Mean bias by category. Bare earth is the only category where the DEMs are underestimating height.

	Bare Earth	Veg < 1m	Veg 1-5m	Veg >5m
LiDAR	.022	-.087	-.166	-.124
SFM	.028	-.124	-.338	-.153

5.5.1 DEM Vertical Accuracy by Vegetation Category

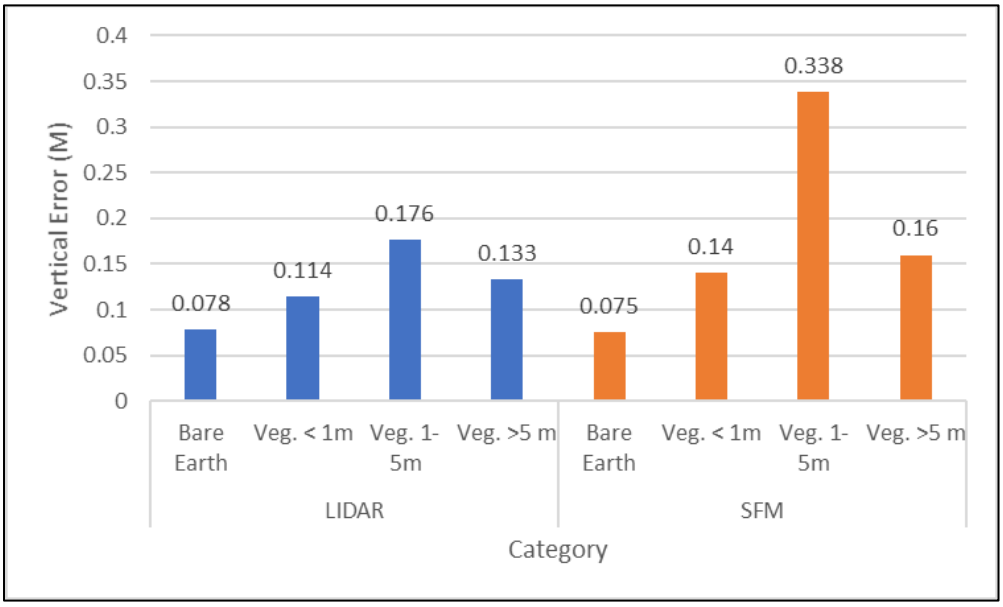

Figure 18. DEM error for all vegetation categories. Similar patterns are shown between both techniques, with vegetation 1-5 meters having the largest vertical error.

Figure 18 is highlighting the pronounced influence of vegetation between 1-5 meters on both LiDAR and SfM. As discussed previously and further examined in section 6, the ground filtering algorithm has difficulties differentiating between vegetation and ground points when there is vegetation in that height range. While the bare earth results for both LiDAR and SfM are very similar, vegetation between 1-5 meters is heavily impacting SfM vertical accuracy.

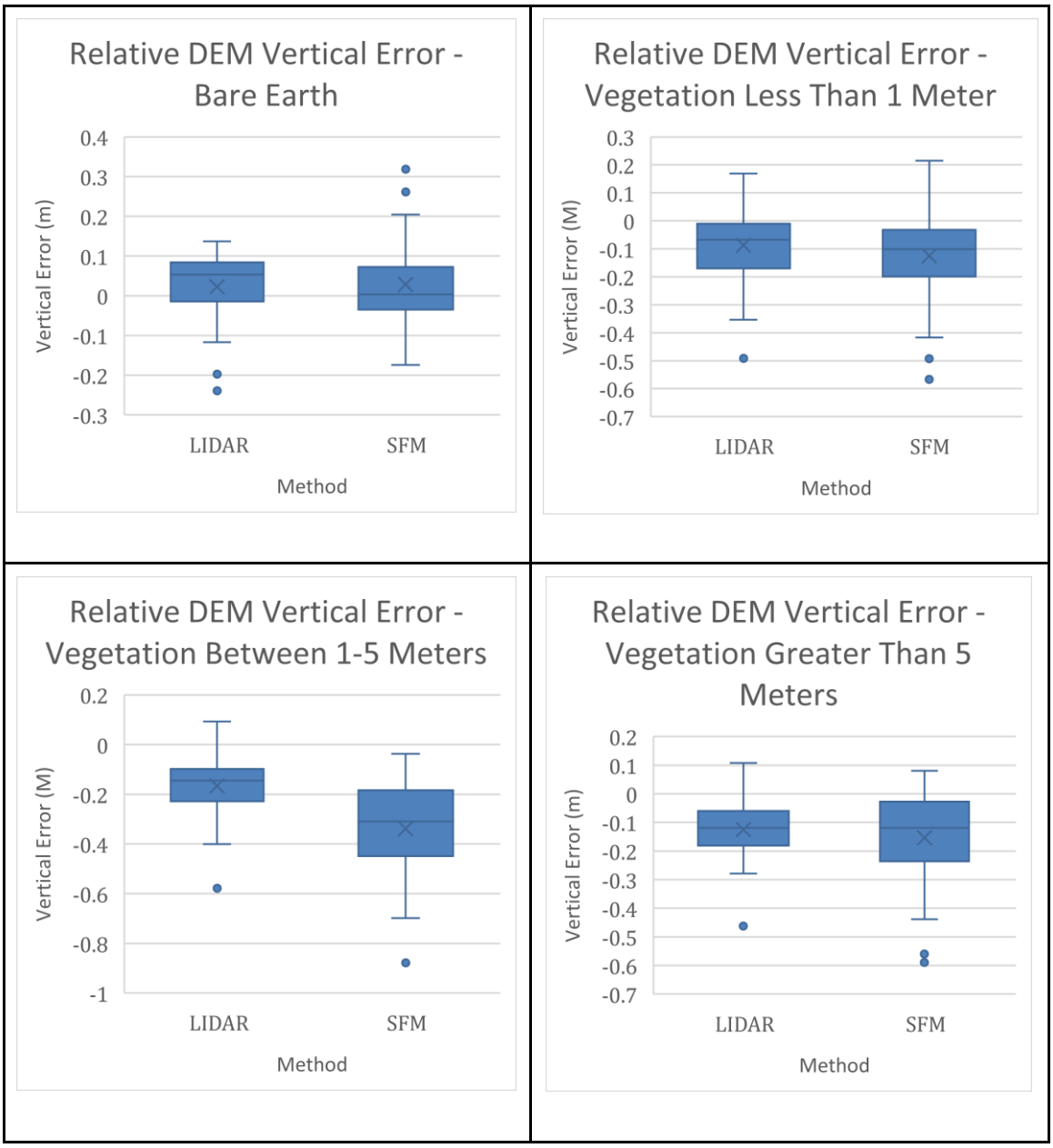

Figure 19. DEM relative vertical error by category (meters). See Appendix C for the numbers of DEM absolute accuracy of all categories.

Figure 19 shows the relative vertical error for each category and highlights how both techniques are underestimating the ground surface elevation when vegetation is present but overestimating the ground surface elevation at bare earth locations. Similarly, Figure 19 also shows the influence of outliers on SfM when compared to LiDAR.

Tables 10 and 11 below show the root mean square error (RMSE) for each category and the RMSE computed at the 95% confidence interval. The analysis highlights the influence of outliers on each method and further shows the influence of vegetation between 1-5 meters. The RMSE results show the oversized impact of vegetation between 1-5 meters on both SfM and LiDAR.

Table 10. DEM RMSE (meters).

	Bare Earth	Veg <1m	Veg 1-5m	Veg >5m
LiDAR	.0922	.153	.212	.1610
SfM	.1135	.188	.398	.2249

Table 11. DEM RMSE at 95% Confidence Interval (meters).

	Bare Earth	Veg <1m	Veg 1-5m	Veg >5m
LiDAR	.1808	.3013	.4173	.3156
SfM	.2224	.3704	.7806	.4409

While the RMSE results show that overall LiDAR has higher accuracy results, the limitations of the ground filtering algorithm are apparent. The DEM vertical accuracies are more similar between SfM and LiDAR when compared to the accuracies of the vertically closest point analysis. This result is showing that despite the higher accuracy of the initial LiDAR point clouds, the inclusion of non-ground points after filtering are impacting the DEM vertical accuracy and therefore increasing the error of the DEM results.

Chapter 6

Discussion

6.1 Processing Parameters

As discussed in section 4.4, adjusting the processing parameters for ground filtering has an effect on vertical accuracy of the interpolated DEM surfaces. Based on our sensitivity analysis, cloth resolution had the greatest impact on filtering results, this result is similar to the findings from Klaptse et al. (2020). Figures 20 and 21 show the effects of cloth resolution changes on DEM outputs. While there are differences throughout the study areas, in the vast majority of cells, the DEM results remain consistent despite variations in the processing parameters. The Figures (20 and 21) compare the adjusted cloth resolution of .1 to the chosen resolution of .2. This adjusted cloth resolution is including more vegetation as ground points for both LiDAR and SfM and as a result, the DEM elevations are higher in the vegetated areas shown.

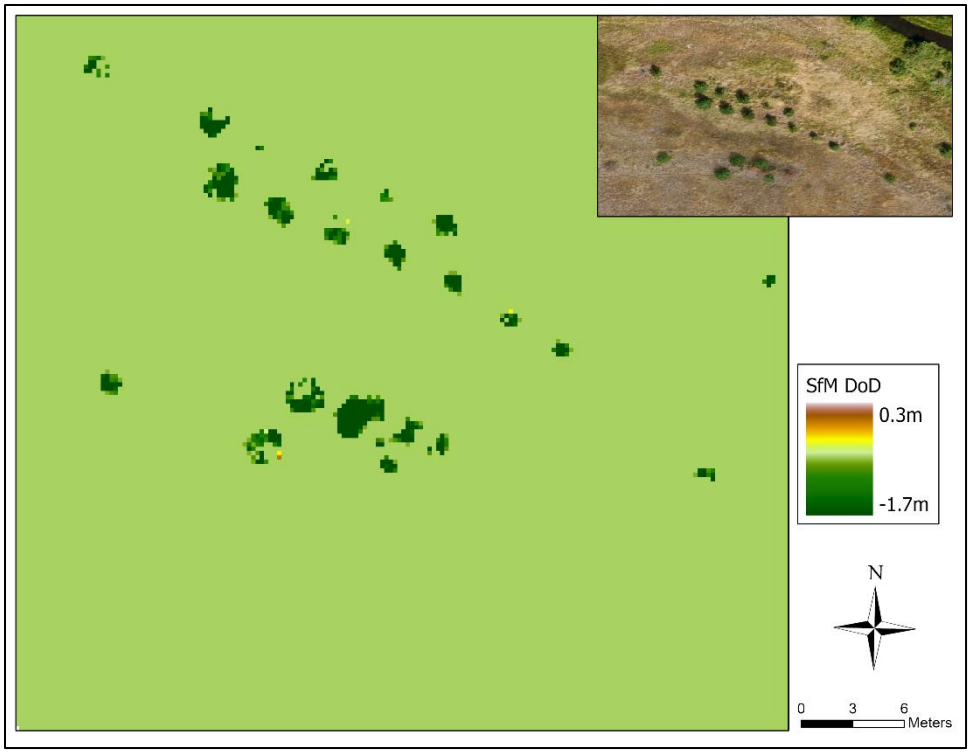

Figure 20. SfM DEM of Difference showing the difference in processing parameters from the CSF algorithm on DEM results. The figure shows cloth resolution of .2 minus the cloth resolution of .1. The higher values show that the cloth resolution of .1 includes more vegetation in the ground points and is resulting in a DEM with higher values in the vegetation.

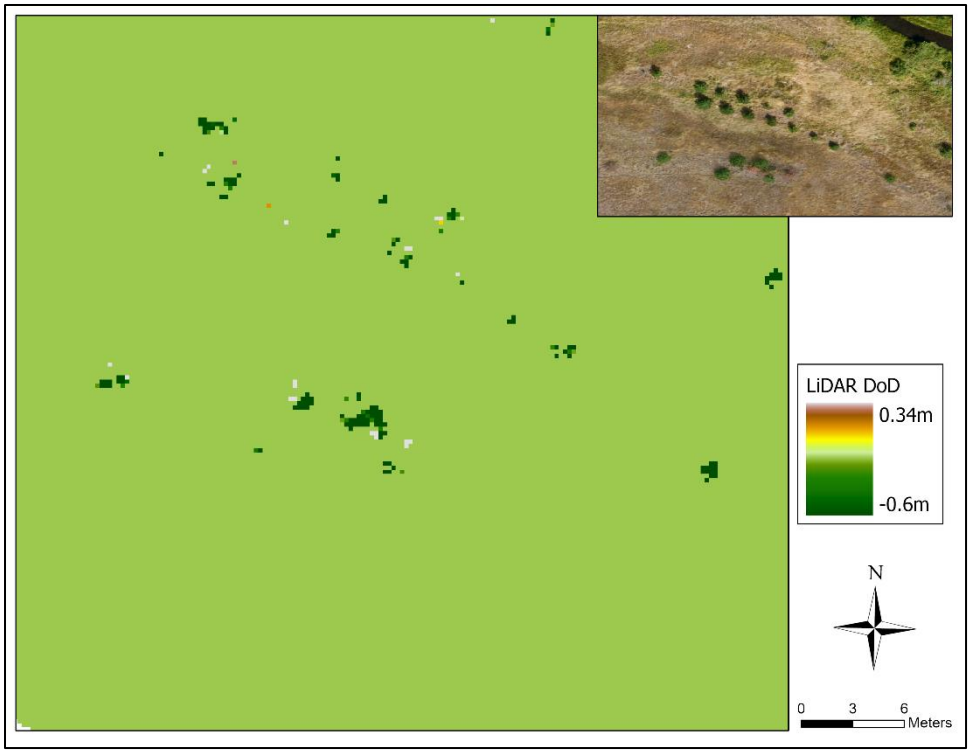

Figure 21. LiDAR DoD showing the difference in processing parameters of the CSF algorithm on DEM results. The figure shows the cloth resolution of .2 minus the cloth resolution of .1.

Examining the filtered point clouds and resulting DEMs it is clear that smaller vegetation features can confuse the algorithm and make it difficult to determine differences between vegetation features and microtopography of actual ground features. Adjusting the filtering parameters can either direct the DEM towards including some vegetation or excluding some microtopography. There is a tradeoff between including microtopography within the site and eliminating vegetation. LiDAR helps eliminate most of these issues because of its ability to reach ground, or closer to ground features, within vegetation. The ground, or closer to ground, points allow the filtering algorithm to

exclude most vegetation points while simultaneously including microtopography within the site.

6.2 Vegetation height and vertical accuracy

Vegetation has a clear impact on the vertical accuracy of both LiDAR point clouds and SfM point clouds with a larger influence on the SfM point clouds than LiDAR. The results clearly show that the LiDAR point clouds return raw vertical values closer to the checkpoint vertical values in varied ground cover. In certain instances, such as bare earth areas, SfM and LiDAR point clouds have similar vertical errors compared to the checkpoints. Overall, vegetation has a negative impact on vertical accuracy on both LiDAR and SfM datasets with varying influence depending on vegetation height.

Figure 22. CC Site 2. For the vertically closest point analysis, the point shown has the highest LiDAR error (.34m) and 5th highest SfM error (.54m).

Figure 23. MFJD Site 2. For DEM results, the point has the highest error for both LiDAR (.57m) and SfM (.87m).

As shown in figure 22, dense grasses impact vertical accuracy of LiDAR to a large degree. The point displayed in Figure 22 is in the vegetation less than 1 meter category. This point has the third highest error for LiDAR DEM checkpoints. It is likely that no LiDAR returns are penetrating the grasses to reach the ground surface and are instead returning values from the grass itself. Therefore, ground filtering likely has little effect on this type of point.

Figure 23 shows the highest SfM point error and is likely caused by a combination of the limitations of SfM point cloud generation and filtering. The point features vegetation between 1-5 meters, which is shown to be the most difficult to

categorize the ground vs. non-ground points. This same point features the highest error for both the SfM and LiDAR DEMs (.87m and .57m, respectively). This result is expected for the SfM DEM but unexpected for the LiDAR DEM because of the low point cloud vertical error (.004m). However, when looking at the thinned point clouds mentioned later in this discussion, thinning of the point cloud shows a large improvement in the DEM accuracy.

Vegetation greater than 5 meters and less than 1 meter has less of an impact on vertical accuracy for SfM point clouds than vegetation between 1-5 meters. This is at least partially explained by the ground filtering algorithm, which is classifying some vegetation points in the 0-5 meter range as ground points but removing points that are above that threshold. Viewing the DEM outputs after ground filtering in Figure 24, it is clear that more vegetation points in the SfM point clouds are being classified as ground points erroneously compared to LiDAR. The same conclusions can be drawn from Figure 25, which shows a cross-section of the DEM elevations through a row of trees and the increase in elevations at the trees for both techniques.

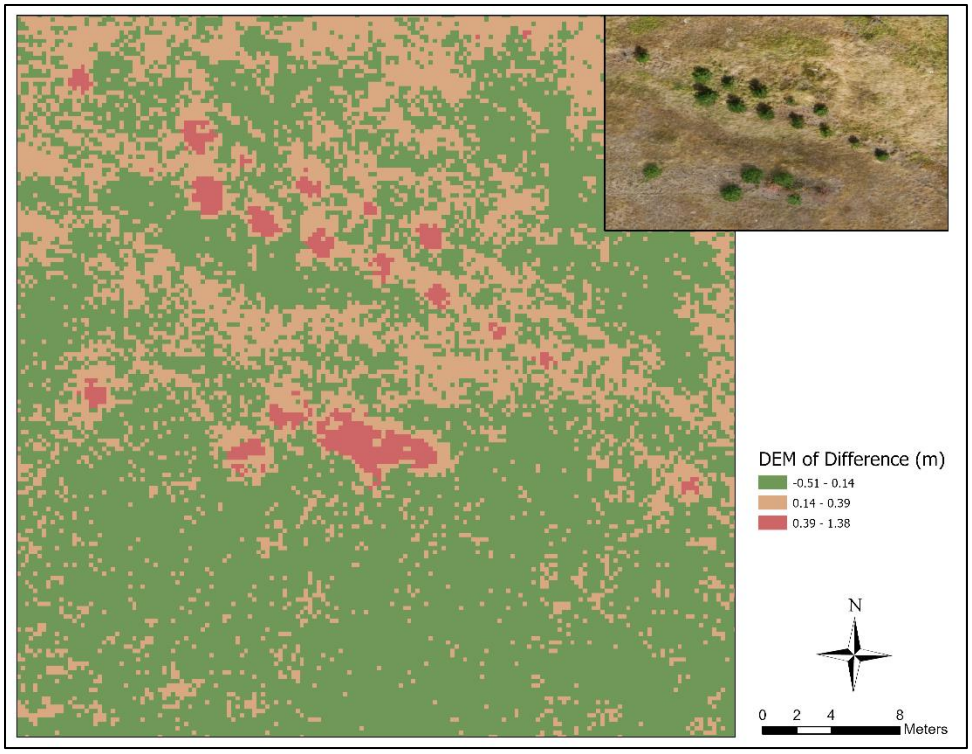

Figure 24. DEM of Difference (DoD) at MFJD site 1. The DoD (SfM – LiDAR) shows the SfM DEM has higher elevation values at the locations of trees because of the misclassification.

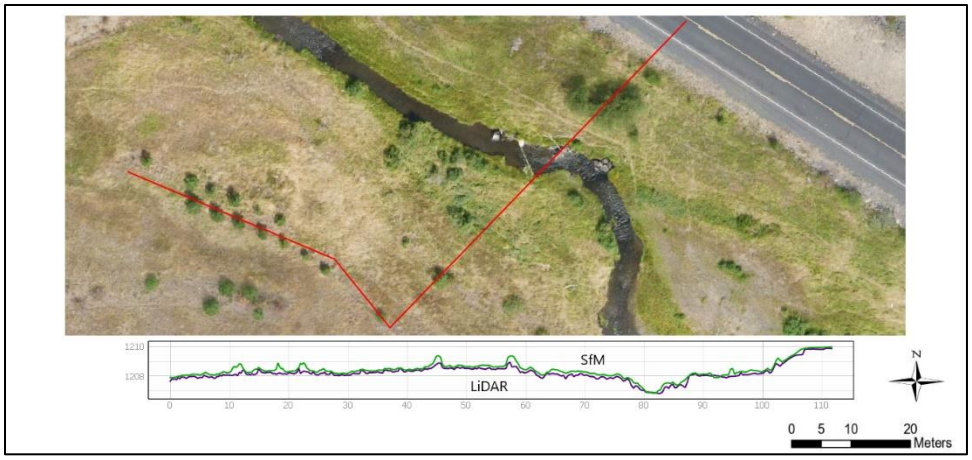

Figure 25. Cross Section Showing the same area at MFJD Site 1. Plotted cross section showing the SfM DEM including more vegetation points as ground points compared to LiDAR.

Checkpoints associated with vegetation between 1-5 meters having the largest vertical error is related to the issues previously discussed about ground filtering. Since these points have vegetation that is further from the actual ground surface, and have some points included in the ground classification, their error values should be higher than vegetation less than 1 meter. It is likely that the filtering algorithm is reaching its limit of classifiying groud points when vegetation somewhere in the 1-5 meter height range is present, which can potentially explain why vegetation greater than 5 meters has less of an effect on vertical accuracy compared to shorter vegetation. This effect is clear when viewing the point clouds at a fine scale. Figure 26 and 27 highlight the inclusion of vegetation as ground points for both SfM and LiDAR, with the effect pronounced further in the SfM point clouds. The figures show how point cloud returns that are approximately 1-2 meters above the ground surface are being included in the filtered returns as ground points. This effect is impacting results in the vegetation 1-5 meter category and likely explains why the category has the highest error values.

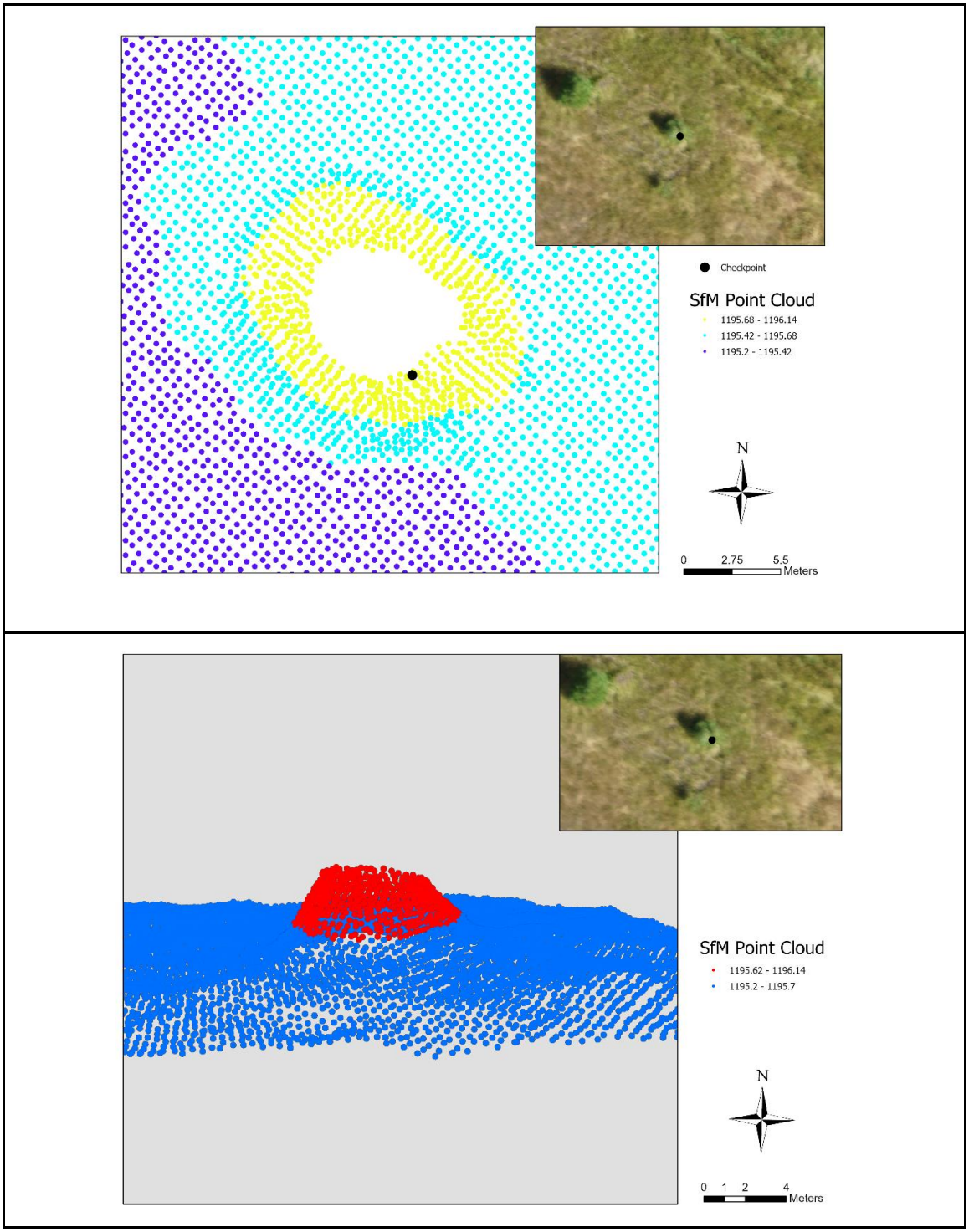
Checkpoint
SfM Point Cloud
1195.68 - 1196.14
1195.42 - 1195.68
1195.2 - 1195.42
N
0 2.75 5.5
Meters
SfM Point Cloud
1195.62 - 1196.14
1195.2 - 1195.7
N
0 1 2 4
Meters

Figure 26. 2D and 3D view of vegetation being included in SfM ground points at a checkpoint location for site MFJD Site 1.

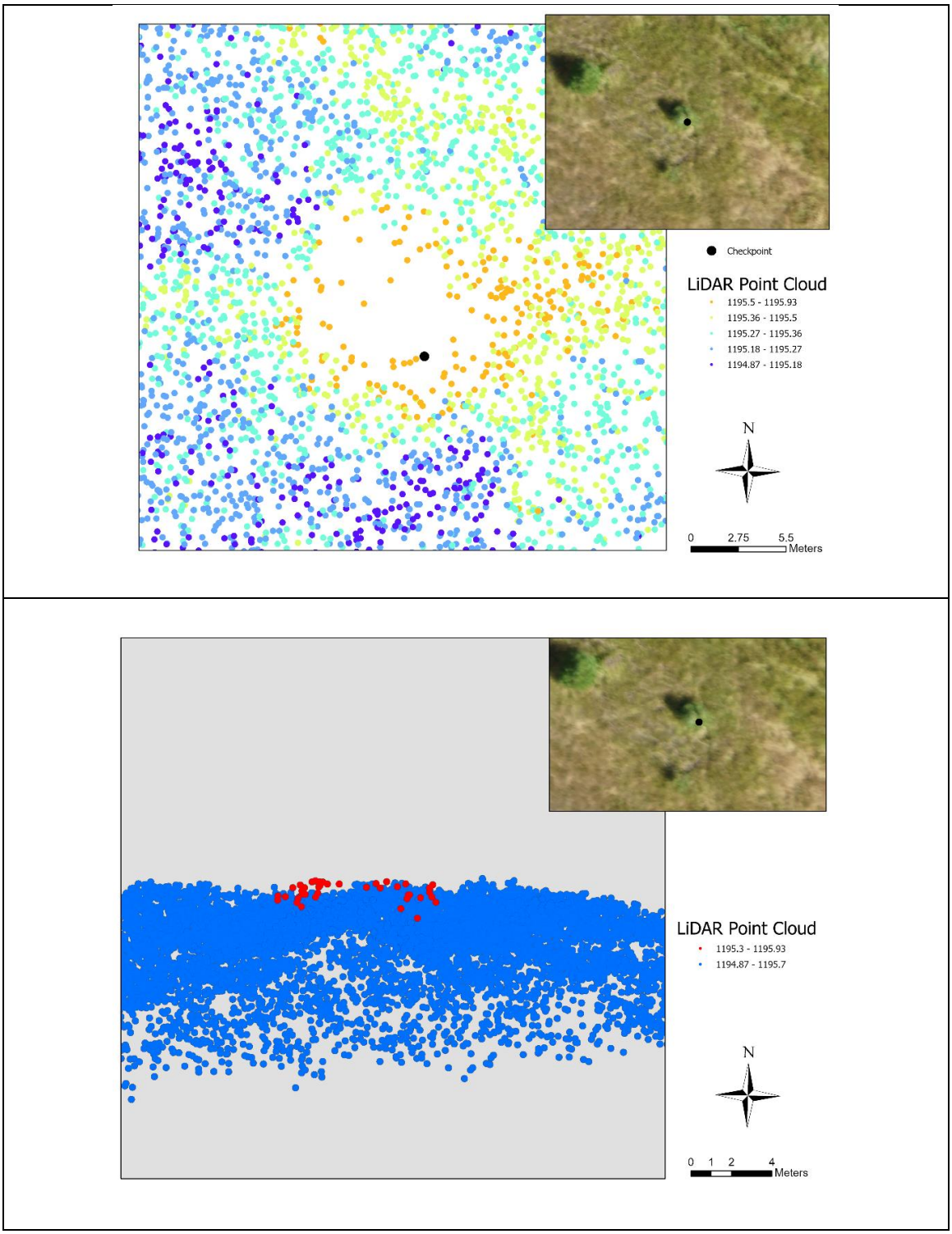

Figure 27. 2D and 3D view of vegetation being included in LiDAR ground points at a checkpoint location for site MFJD Site 1.

The ring of no data near the checkpoint shows that the upper portion of the vegetation associated with the checkpoint is being removed from the ground classification, while the edges of the vegetation are still included. These erroneous ground points are causing the vertical error to be increased. Figure 27 highlights the less pronounced effect with LiDAR. This effect is emphasized in the DEM RMSE results when compared to the vertically closest point results. If filtering was more accurate in capturing just ground points, the results between the two analyses should be closer. However, looking at the LiDAR average vertical error by category for both types of analysis, it is clear that the inclusion of erroneous points are greatly impacting the DEM results. For LiDAR RMSE results in the vegetation between 1-5 meters, the vertically closest point average is .1046 meters while the DEM average error is .212 meters.

The effect of vegetation on vertical values becomes even clearer when viewing the checkpoints associated with the highest error values. For SfM, the 11 highest error points are from vegetated points and only 1 of the 23 highest error points is a bare earth point. For LiDAR, the 15 highest error points are associated with vegetation and only 1 of the 29 highest error points is a bare earth point.

The results show that low-lying, dense vegetation has a greater impact on SfM vertical accuracy when compared to LiDAR. Higher vegetation, both mature deciduous and coniferous trees, have less of an impact on SfM vertical accuracy than vegetation between 1-5 meters in height. This suggests that study areas that encompass ecosystems

with little understory could be good candidates for SfM DEMs and the added expense of LiDAR may not be necessary. For sites with dense understory vegetation, typically grasses and shrubs, SfM is not ideal and LiDAR should be the default system choice.

6.3 Thinning Point Clouds and DEM results

Because of the erroneous inclusion of non-ground points in the ground filtered point cloud I completed further analysis to determine the effects of further filtering on DEM results. After point clouds are filtered for ground vs. non-ground points, the resulting ground points are then thinned using two different grid sizes (.25 and .5 meters) with the ArcGIS thin LAS tool. The thinning algorithm allows the user to choose the points included in the thinned point cloud such as average height of the points within the grid size or, as I chose, the lowest point elevation with the grid. Yilmaz et al. (2021) analyzed the effects of point density on DEM accuracy using SfM point clouds and found that optimum results were achieved with lower-density point clouds. Results below show the differences in DEM results for each category. Figures 28 and 29 show the increase in overall vertical accuracy with thinning for both SfM and LiDAR and the decrease in the number of outliers.

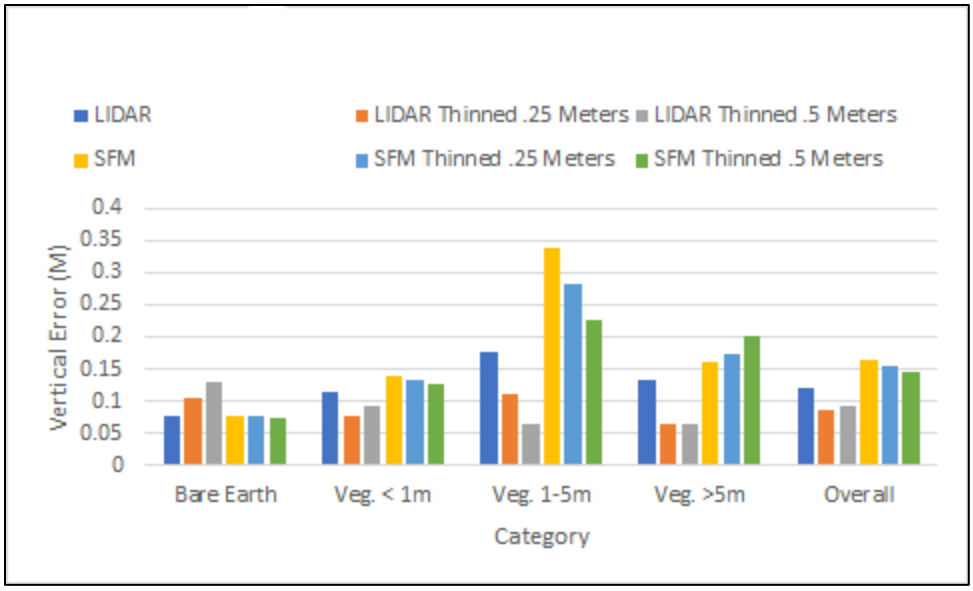

Figure 28. DEM absolute error by category and thinning resolution.

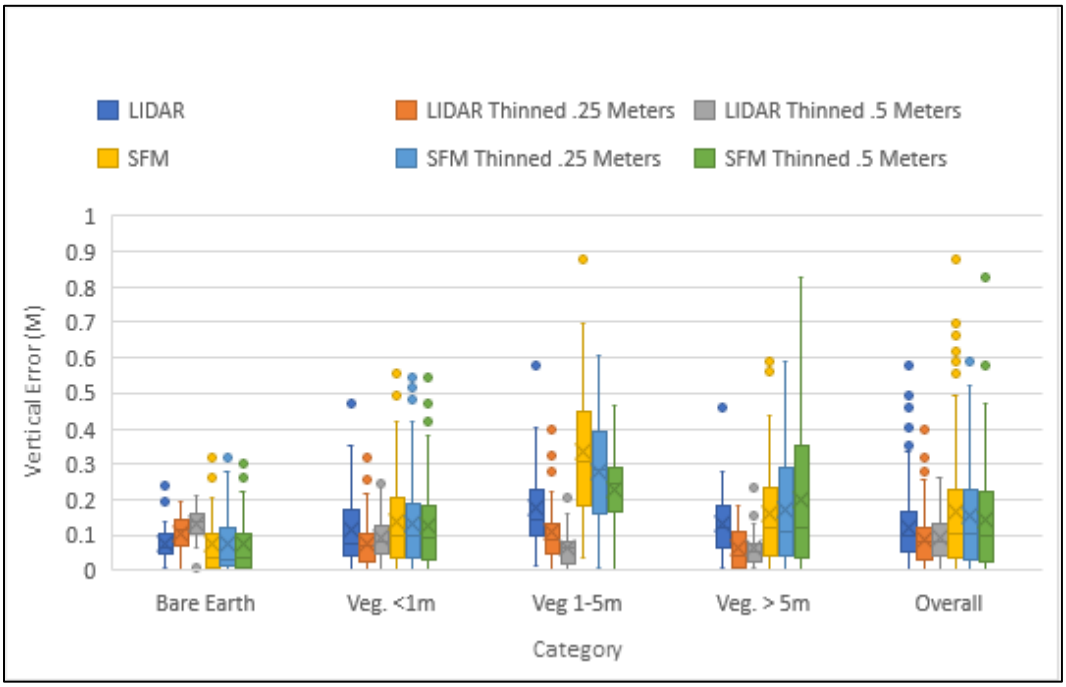

Figure 29. DEM absolute accuracy by category and resolution. Overall, the number of outliers are decreased with thinning.

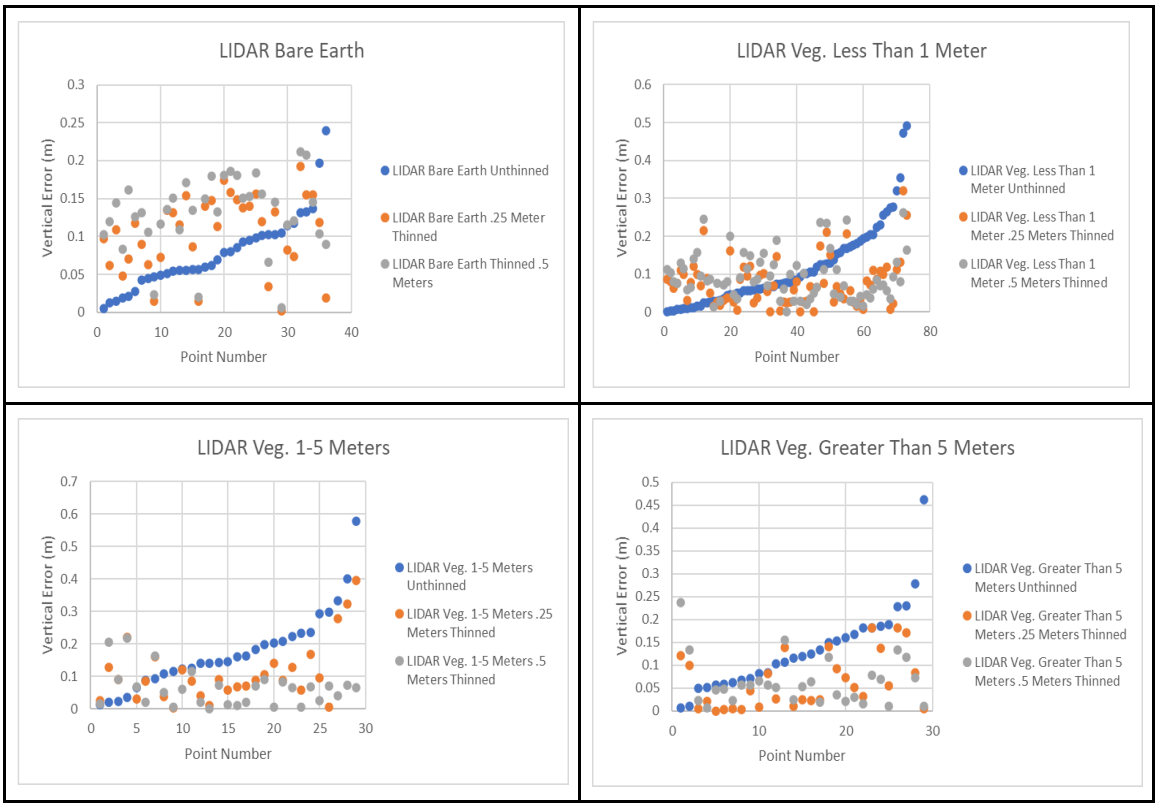

Figure 30. LIDAR DEM Scatter plot comparison. The scatter plots are arranged from lowest to highest vertical error for the unthinned point clouds for each category.

When looking at the LiDAR bare earth DEM values in Figure 28, it is clear that thinning the point clouds largely introduces more error. This is likely due to the DEM interpolating values from fewer overall points and is also from the thinning method, which includes only the lowest values in each grid of the chosen size. Figures 30 and 31 show the scatter plot of points by category arranged from the lowest to highest error for the original DEM values. The trends show the overall increase in accuracy with thinning.

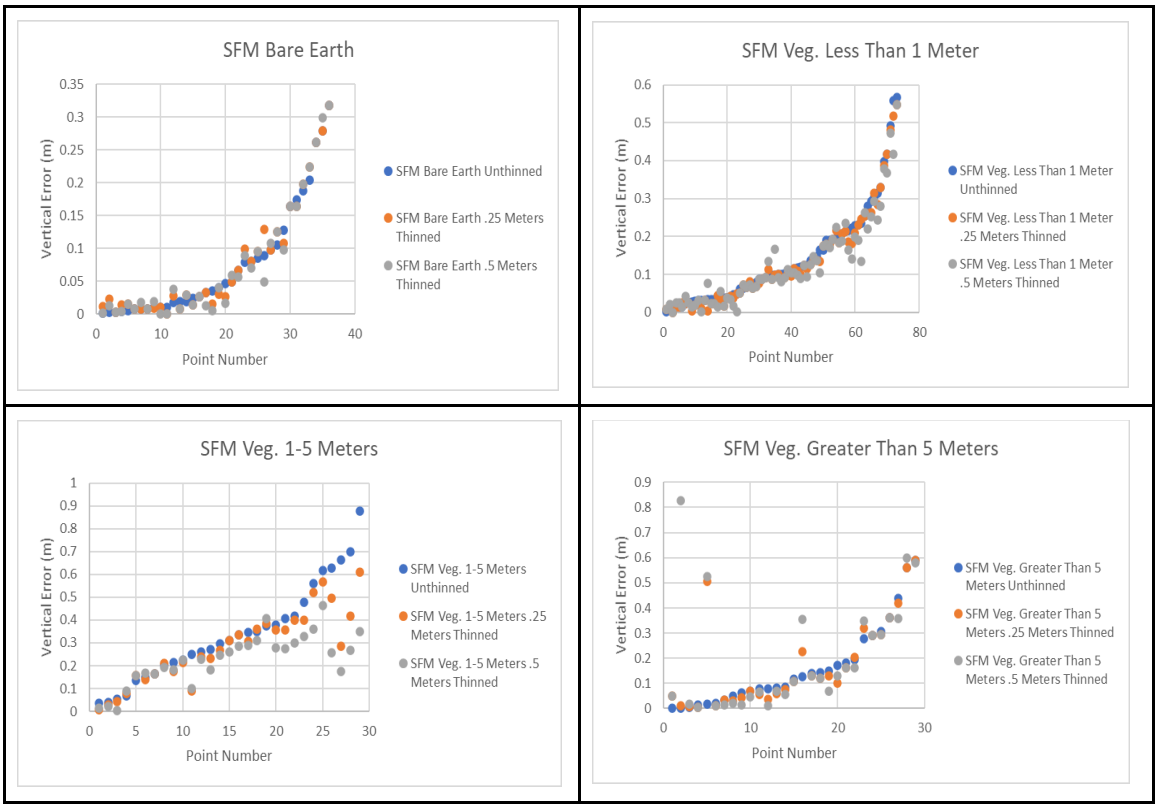

Figure 31. SFM DEM Scatter plot comparison. The scatter plots are arranged from lowest to highest vertical error for the unthinned point clouds for each category.

Table 12. RMSE for DEMs Thinned at .25 and .5 Meters (meters).

Method	**Overall**	**Bare Earth**	**Veg <1m**	**Veg 1-5m**	**Veg >5m**
LiDAR .25m Thinned	.109	.115	.098	.143	.086
LiDAR .5m Thinned	.109	.138	.110	.083	.081
SfM .25m Thinned	.213	.116	.181	.322	.242
SfM .5m Thinned	.203	.115	.170	.252	.292

Table 12 shows the varying impact on DEM results and the differences in thinning on LiDAR and SfM DEM results. For LiDAR, the thinned point clouds had an overall decrease in vertical error with the .5 meter thinning having the lowest overall RMSE (.109 meters). The same is true for SfM results, with .5 meter thinning having the lowest overall RMSE (.203 meters). When broken into land cover categories, the results show differences in the vertical error. LiDAR bare earth checkpoints show a steady increase in vertical error with thinning, while SfM stays fairly consistent. For vegetation less than 1 meter, thinning at .25 meters decreased the vertical error for both LiDAR and SfM. Vegetation between 1-5 meters had a significant decrease in vertical error with

thinning for both LiDAR and SfM. For vegetation greater than 5 meters, LiDAR had a significant decrease in vertical error with thinning while SfM vertical error increased slightly.

The inclusion of microtopography in the DEMs while simultaneously removing vegetation returns that are being classified as ground is a tradeoff and difficult to completely remedy. While thinning clearly decreases the vertical error at the checkpoints, it is also removing some microtopography from the model and is smoothing the results. This evidence of smoothing and the resulting DEM removing microtopography is clear when looking at the bare earth points for LiDAR. The thinned point clouds have eliminated points that more accurately model the surface and therefore increase the vertical error. While in vegetated areas, the thinned points clouds increase accuracy by eliminating the points that are erroneously included in the ground classification. Finding the balance between inclusion of microtopography and exclusion of vegetation is difficult and could be further investigated by further adjusting the thinning grid sizes. A semi-automated approach that masks flat areas from thinning could yield a good compromise between leaving microtopography and eliminating vegetation being included in ground points.

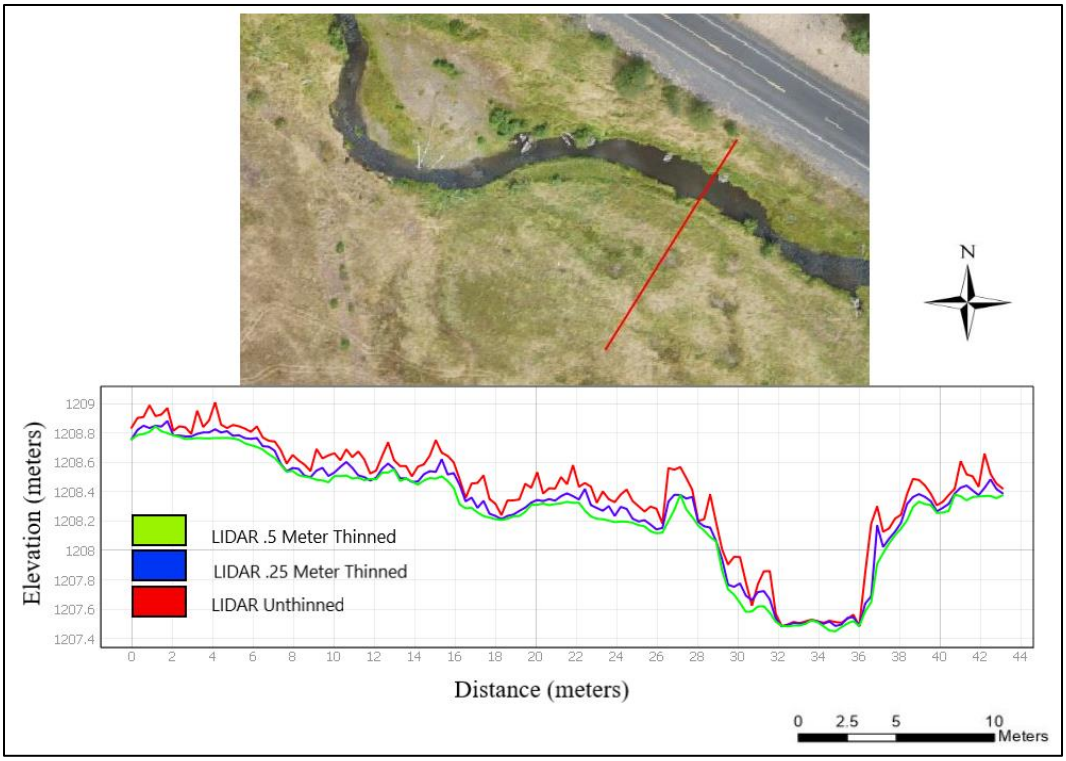

Figure 32. Cross section from MFJD Site 1 highlighting the effect of point cloud thinning and on DEM results.

Figure 32 highlights the smoothing effect on DEMs from point cloud thinning. The unthinned point cloud is including some erroneously classified points, while the thinned point clouds are ignoring some features that should likely be included in the ground classification.

The results presented in the thinning analysis show that the .5 meter grid size thinned point clouds provide the lowest overall error. While the previous discussion on inclusion of microtopography could be further examined, the results should be viewed in the context of comparison with existing methods. Existing methods using ground-based surveys rely heavily on interpolation for DEM creation because of the spacing between each topographic point collected. Previous ground-based surveys have a range of point

density depending on site complexity but typically range from .1 points per m^2 to .4 points per m^2 (Rosgen et al. 2018). In comparison, thinned point clouds would still have much higher point density to interpolate DEMs compared to ground-based surveys and the user can assume that the microtopography inclusion is likely higher. With ground filtered points thinned at the .5 meter grid size, point densities at our study sites range from 3.1-3.4 points per m^2. While these densities are much less than the unthinned point clouds, their densities are still much greater than existing ground-based methods and can provide the user with much higher detail for DEM analysis. With RMSE values for LiDAR and SfM point clouds thinned at .5 meter grid size averaging .11 meters and .20 meters respectively, both techniques could be considered useful depending on the application. Because of the decrease in RMSE with point cloud thinning, it would be a recommended step for DEM processing in vegetated floodplain terrain for both LiDAR and SfM in the future.

6.3 Further Study

This study has provided insight into the strengths and weaknesses of both UAV LiDAR and SfM point cloud accuracy in vegetated study areas. One area that could be further studied is the inclusion of oblique imagery added to SfM acquisition. Our platform featured a nadir camera without the possibility of including oblique imagery because of the fixed mounting platform of the camera. Oblique imagery has been shown to increase ground point returns (Nesbit et al. 2019) and would likely increase the number of ground points included in the final point cloud by reducing data gaps below vegetation.

What became apparent during analysis is the need for development of ground filtering algorithms specifically designed for SfM point cloud processing. The extreme density of SfM point clouds can limit processing speeds as well as complicate the algorithms determining ground vs. non-ground points. Binning algorithms to reduce the total number of points in a point cloud can help alleviate the processing issues but do not address the filtering of point clouds into ground vs. non-ground points.

It is clear that filtering is a major limitation for SfM and LiDAR DEM vertical accuracy. This is apparent when comparing the accuracy of the initial point cloud vertical accuracy and DEM vertical accuracy. The erroneous inclusion of non-ground points is difficult to remedy and will likely be addressed in future research. There are several directions this analysis can take, one being thinning of point clouds prior to filtering, which may alleviate some of the erroneous non-ground points being included in the ground classification. Another is further testing of thinning grid sizes and the effect on DEM results. Ground filtering algorithms are continually being developed and with the expansion and interest in UAV topographic mapping it is likely that they will be improved.

Chapter 7

Conclusion

The specific goals of my research were to: 1) assess the vertical accuracy of UAV-LiDAR and SfM point clouds in the context of floodplains 2) assess the vertical accuracy of UAV-LiDAR and SfM derived DEMs and 3) give recommendations to future practitioners about each technique.

Overall, this study has shown the strengths and weaknesses of UAV-LiDAR and SfM in the context of floodplains. LiDAR was shown to provide more accurate overall point cloud elevations and resulting DEMs. In bare earth locations, SfM and LiDAR provide similar DEM accuracy as expected. In vegetated areas, LiDAR provides higher accuracy results compared to SfM. Both techniques show varying accuracy depending on vegetation height. Vegetation within the 1-5 meter range above the ground surface is contributing the largest source of error in vertical accuracy. Vegetation less than 1 meter and greater than 5 meters has less of an impact on vertical accuracy compared to vegetation between 1-5 meters but still contribute to overall error. The difficulty of these sites for both methods should be not understated and all four sites are inherently challenging to both techniques. LiDAR and SfM are both known to be impacted by dense vegetation, which all the study sites feature, and overall the results from both techniques show relatively high accuracy compared to their acquistion cost.

Ground filtering was shown to not accurately represent the ground surface and is instead including some vegetation points in the filtered results. This result is highlighted by the difference in the vertically closest point results and the DEM results, with an

increased emphasis on LiDAR. While the LiDAR point clouds are providing returns that are overall fairly accurate, the inclusion of erroneous vegetation results in the filtered point clouds are causing the DEM vertical accuracy to decrease. Thinning of the point clouds prior to DEM creation is shown to increase vertical accuracy, with the caveat being that microtopography is somewhat removed from the DEM. Depending on the needs of a specific use, a practitioner can err on the side of vegetation and microtopography inclusion or vice versa.

For overall effort and time, the two techniques discussed have similar requirements with SfM needing slightly more processing and field-based steps. SfM with ground control points requires both setting and measuring GCP's throughout each study area and then processing the imagery with GCP's to acquire a georeferenced point cloud. LiDAR requires more equipment, with an onboard GNSS receiver and INS whereas for SfM the camera and GCP's negate the need for either. In terms of cost, SfM is much less expensive and could be completed with equipment costing less than one thousand dollars. In comparison, UAV-LiDAR sensors cost roughly one thousand dollars a day to rent and can be purchased for several ten of thousands of dollars. The increased cost associated with LiDAR can be prohibitve to some practictioners.

Based on our analysis, LiDAR is the recommended sensor in typical floodplain habitats. Because floodplains typically feature vegetation within all height classes presented in our analysis, SfM is not recommended. However, it is conceivable that certain ecosystems may contain vegetation that is advantageous for SfM such as sparse mature trees and little to no vegetation within 1-5 meters in height. As such, the

individual practitioner should use their knowledge of a specific ecosystem to determine if SfM is applicable for their needs. Likewise, the higher error associated with SfM could be acceptable for many projects and can still be considered a useable method available at a much lower cost than LiDAR systems. SfM should not be entirely discredited and the results show that while LiDAR produces overall higher accuracy DEMs, SfM is producing quality results at a much lower cost. With the high level of interest in utilizing UAVs for topographic mapping and the evolving nature of ground filtering algorithms improving their classification it is likely that both techniques will improve in accuracy and usefulness in the near future.

References

Agisoft Metashape Professional (Version 1.5.5). 2020. [computer software]. St. Petersburg, Russia. https://www.agisoft.com/.

American Society for Photogrammetry and Remote. 2015. ASPRS Positional Accuracy Standards for Digital Geospatial Data. doi:10.14358/PERS.81.3.A1-A26.

Bangen, Sara G, Joseph M Wheaton, Nicolaas Bouwes, Boyd Bouwes, and Chris Jordan. 2014. "A Methodological Intercomparison of Topographic Survey Techniques for Characterizing Wadeable Streams and Rivers." Geomorphology 206. Elsevier B.V.: 343–61. doi:10.1016/j.geomorph.2013.10.010.

Bonneville Power Administration. 2014. Action Effectiveness Monitoring Program. Portland, OR. https://www.monitoringresources.org/Resources/Program/Detail/58.

Carrivick, Jonathan L, and Mark W Smith. 2019. "Fluvial and Aquatic Applications of Structure from Motion Photogrammetry and Unmanned Aerial Vehicle / Drone Technology." WIREs Water 6: 1–17. doi:10.1002/wat2.1328.

Dietrich, James T. 2016. "Geomorphology Riverscape Mapping with Helicopter-Based Structure-from-Motion Photogrammetry." Geomorphology 252. Elsevier B.V.: 144–57. doi:10.1016/j.geomorph.2015.05.008.

ESRI. 2020. ArcGIS for Desktop Advanced (version 10.7) [computer software]. Redlands, CA. http://www.esri.com/software/arcgis/arcgis-for-desktop.

Evans, J. S., & Hudak, A. T. 2007. A multiscale curvature algorithm for classifying discrete return LiDAR in forested environments. IEEE Transactions on Geoscience and Remote Sensing, 45(4), 1029–1038. http://doi.org/10.1109/TGRS.2006.890412

Fonstad, Mark A, James T Dietrich, Brittany C Courville, Jennifer L Jensen, and Patrice E Carbonneau. 2013. "Topographic Structure from Motion : A New Development in Photogrammetric Measurement." Earth Surface Processes and Landforms 38: 421–30. doi:10.1002/esp.3366.

Hodgson, Michael E, and Patrick Bresnahan. 2004. "Accuracy of Airborne Lidar-Derived Elevation : Empirical Assessment and Error Budget." Photogrammetric Engineering & Remote Sensing 70 (3): 331–39.

Klápště, Petr, Michal Fogl, Vojtěch Barták, Kateřina Gdulová, Rudolf Urban, Vítězslav Moudrý, Petr Klápště, et al. 2020. "Sensitivity Analysis of Parameters and Contrasting Performance of Ground Filtering Algorithms with UAV Photogrammetry-Based and LiDAR Point Clouds." Taylor & Francis. doi:10.1080/17538947.2020.1791267.

Kucharczyk, Maja. 2017. "UAV-LiDAR and Structure from Motion Photogrammetry: Spatial Accuracy in Vegetated Terrain." Thesis - University of Calgary, 92.

L3 Harris Geospatial. 2021. Exelis Visual Information Service (version 4.8) [computer software]. Boulder, CO. https://www.l3harrisgeospatial.com/Software-Technology/ENVI.

Litchi. 2020. [computer software]. Fly Litchi. London, UK. https://flylitchi.com/.

National Geodetic Survey. 2020. OPUS: Online Positioning User Service. https://www.ngs.noaa.gov/OPUS/about.jsp.

Nesbit, Paul Ryan, and Christopher H Hugenholtz. 2019. "Enhancing UAV – SfM 3D Model Accuracy in High-Relief Landscapes by Incorporating Oblique Images." Remote Sensing, 1–24. doi:10.3390/rs11030239.

Phoenix LiDAR Systems. 2020. [computer software]. Phoenix LiDAR Flight Planner. Austin, TX. https://www.phoenixlidar.com/flightplan/.

Renslow, Michael S. 2012. Manual of Airborne Topographic Lidar. American Society for Photogrammetry Remote Sensing.

Roni, Phil, Chris Clark, Michelle Krall, Shelby Burgess, and Kai Ross. 2020. "Action Effectiveness Monitoring 2019 Annual Report," no. 2016.

Rosgen, Dave, Ron Pierce, Jim Nankervis, Ryan Kovach, Michael Geenen, and Taillacq Andrea. 2018. "A Technical Review of the Columbia Habitat Monitoring Program's Protocol, Data Quality & Implementation." Bonneville Power Administration.

Roussel J, Auty D, Coops NC, Tompalski P, Goodbody TR, Meador AS, Bourdon J, de Boissieu F, Achim A (2020). "lidR: An R package for analysis of Airborne Laser Scanning (ALS) data." Remote Sensing of Environment, 251, 112061. doi: 10.1016/j.rse.2020.112061, https://www.sciencedirect.com/science/article/pii/S0034425720304314.

Rusnak, Milos, Ján Sládek, Anna Kidová, and Milan Lehotský. 2018. "Template for High-Resolution River Landscape Mapping Using UAV Technology." Measurement 115: 139–51. doi:10.1016/j.measurement.2017.10.023.

Simpson, Chase. 2018. "A Multivariate Comparison of Drone-Based Structure from Motion and Drone- Based Lidar for Dense Topographic Mapping Applications." Thesis - Oregon State University, 50.

Snavely, Noah, Steven M Seitz, and Richard Szeliski. 2006. "Photo Tourism : Exploring Photo Collections in 3D" 1 (212): 835–46.

Tan, Yumin, Shuai Wang, Bo Xu, and Jiabin Zhang. 2018. "An Improved Progressive Morphological Filter for UAV-Based Photogrammetric Point Clouds in River Bank Monitoring." ISPRS Journal of Photogrammetry and Remote Sensing 146: 421–29. doi:10.1016/j.isprsjprs.2018.10.013.

Trimble. 2020. [computer software]. Trimble Business Center. https://heavyindustry.trimble.com/en/products/trimble-business-center.

Westoby, M J, J Brasington, N F Glasser, M J Hambrey, and J M Reynolds. 2012. "'Structure-from-Motion' Photogrammetry: A Low-Cost , Effective Tool for Geoscience Applications." Geomorphology 179. Elsevier B.V.: 300–314. doi:10.1016/j.geomorph.2012.08.021.

Yilmaz, Cigdem Serifoglu and Oguz Güngör 2021. "The Effect of Point Density on Point Cloud Filtering Performance." Turkish Journal of Remote Sensing and GIS, 2(1), pp.41-46.

Yilmaz, Cigdem Serifoglu, Volkan Yilmaz, and Oguz Güngör. 2018. "Investigating the Performances of Commercial and Non-Commercial Software for Ground Filtering of UAV-Based Point Clouds." International Journal of Remote Sensing 00 (00). Taylor & Francis: 1–27. doi:10.1080/01431161.2017.1420942.

Zeybek, Mustafa. 2019. "Point Cloud Filtering on UAV Based Point Cloud" c: 99–111. doi:10.1016/j.measurement.2018.10.013.

Zhang, Wuming, Jianbo Qi, Peng Wan, Hongtao Wang, Donghui Xie, and Xiaoyan Wang. 2016. "An Easy-to-Use Airborne LiDAR Data Filtering Method Based on Cloth Simulation," 1–22. doi:10.3390/rs8060501.

Appendix A: RMSE results from Aigsoft Metashape processing.

Site	RMSE X (CM)	RMSE Y (CM)	RMSE Z (CM)	RMSE Total (CM)
MFJD Site 1	1.73	1.31	.31	2.19
MFJD Site 2	1.39	1.71	.78	2.34
CC Site 1	1.16	1.21	.36	1.72
CC Site 2	1.12	1.12	.95	1.85

Appendix B: RMSE results from LiDAR processing.

Site	RMSE X (CM)	RMSE Y (CM)	RMSE Z (CM)	RMSE Total (CM)
MFJD Site 1	1.4	.7	1.0	1.1
MFJD Site 2	.8	1.1	.5	1.5
CC Site 1	1.0	2.1	.6	1.6
CC Site 2	1.1	2.1	.6	1.5

Appendix C: DEM absolute accuracy average all categories and thinning grid size (meters).

Method	Overall	Bare Earth	Veg. < 1m	Veg. 1-5m	Veg. > 5m
LIDAR	.12	.078	.114	.176	.133
LIDAR .25m	.087	.105	.077	.111	.063
LIDAR .5m	.091	.131	.093	.063	.063
SFM	.164	.075	.14	.338	.16
SFM .25m	.154	.078	.133	.281	.173
SFM .5m	.145	.074	.126	.227	.2